APEX2 proximity biotinylation reveals protein dynamics triggered by B cell receptor activation

Authors:

Luqman O Awoniyi[1,2], Vid Šuštar[1], Sara Hernández-Pérez[1,2,], Marika Vainio[1,2], Alexey V Sarapulov[1,2], Petar Petrov[1,2] and Pieta K Mattila[1,2*]

Affiliations:

[1] Institute of Biomedicine and MediCity Research Laboratories, University of Turku, Turku, Finland

[2] Turku Bioscience, University of Turku and Åbo Akademi University, Turku, Finland

*** Correspondence:**

Corresponding author

Pieta K Mattila

pieta.mattila@utu.fi

Keywords: Immunology, B cells, BCR, antigen receptor, receptor signaling, proximity proteomics

ABSTRACT

B lymphocytes form a central part of the adaptive immune system, helping to clear infections by mounting antibody responses and immunological memory. B cell activation is critically controlled by a specific antigen receptor, the B cell receptor (BCR), which triggers a complex, multibranched signaling cascade initiating various cellular changes. While parts of these pathways are reasonably well characterized, we still lack a comprehensive protein-level view of the very dynamic and robust cellular response triggered by antigen engagement. Ability to track, with sufficient kinetic resolution, the protein machineries responding to BCR signaling is imperative to provide new understanding into this complex cell activation event. We address this challenge by using APEX2 proximity labeling technique, that allows capture a major fraction of proteins in a given location with 20nm range and 1min time window, and target the APEX2 enzyme to the plasma membrane lipid raft domain, where BCR efficiently translocates upon activation. Our data provides unprecedented insights into the protein composition of lipid raft environment in B cells, and the changes triggered there upon BCR cross-linking and translocation. In total, we identified 1677 proteins locating at the vicinity of lipid raft domains in cultured mouse B cells. The data includes a majority of proteins known to be involved in proximal BCR signaling. Interestingly, our differential enrichment analysis identified various proteins that underwent dynamic changes in their localization but that had no previously known linkage to early B cell activation. As expected, we also identified, for example, a wealth of proteins linked to clathrin-mediated endocytosis that were recruited to the lipid rafts upon cell activation. We believe that his data serves as a valuable record of proteins involved in BCR activation response and aid various future studies in the field.

INTRODUCTION

B lymphocytes form a critical branch of the adaptive immune system by differentiating into the antibody producing plasma cells after recognition of specific antigens via their characteristic B cell receptor (BCR). BCR signaling is a robust trigger that leads to detectable phosphorylation of, for instance, the downstream kinases within seconds or minutes, as well as to rapid internalization of the receptors detectable already after 5-10 min of activation. Numerous studies on BCR signaling have sketched a picture of multi-branched signaling network that triggers not only the signaling cascades to change the transcriptional program but also other cellular machineries such as cytoskeleton reorganization, endocytosis and vesicle transport, as well as protein degradation (Kuokkanen et al., 2015; Kwak et al., 2019). Engagement of such a vast variety of, often interlinked, cellular pathways have challenged our understanding of the early events of B cell activation. One of the major limitations has been the inability to study the combinations of cellular changes in required spatial and temporal resolution.

A popular and efficient way of identifying novel players in given cellular pathways is proteomics. Traditional proteomic approaches, relying on co-immunoprecipitations and organelle purification, have significant challenges in capturing protein interactions or recruitment events with transient nature or fast dynamics, and also occur in the test tube instead inside cells. In recent years, promiscuous proximity labeling techniques have become a powerful tool for mapping protein-protein interactions in cellular environment. These techniques are typically based on *in situ* biotinylation, which is triggered by enzymes generating short-lived biotin radials to the immediate molecular environment (Samavarchi-Tehrani et al., 2020). The two most commonly used enzymes in proximity labeling are BioID/BirA* and APEX, and their variants (Rhee et al., 2013; Roux et al., 2012). The fastest and most efficient biotinylation is reached with use of APEX2 (Lam et al., 2015), where the biotinylation reaction time is 1 min, while the fastest version of BioID, TurboID, requires 10 min for biotinylation (Doerr, 2018), making the method unsuitable to capture signaling events with high dynamics.

APEX2 has been successfully used to identify protein environments in various cellular compartments as its biotinylation radius is 20 nm. For instance APEX/2 had been used to map proteomes of mitochondrial matrix, mitochondrial intermembrane space and primary cilia,(Hung et al., 2014; Mick et al., 2015; Rhee et al., 2013). In addition, due to APEX2 fast labeling, Paek et al., 2017 used APEX2 to track GPCR signaling and internalization with high spatial resolution (Paek et al., 2017). Recently APEX2

was targeted to different compartment such as mitochondrial matrix, endoplasmic reticulum (ER), nucleus and cytosol to identify RNAs localized to these compartment with high specificity and sensitivity (Kaewsapsak et al., 2017). In order to detect changes in the signaling environment, APEX2 can be fused to a protein of interest or directed to a compartment of interest. While expressing APEX2 as a fusion partner of a particular signaling protein can be technically challenging and also potentially compromise the protein function, targeting the biotinylating enzyme to the cellular compartment of interest could provide more physiological readout. One of the first cellular changes triggered by the BCR engagement is the translocation of the receptor into so-called lipid rafts, membrane domains rich in cholesterol, accompanied by fusion and/or enlargement of these domains (Gupta & DeFranco, 2003). Lipid rafts have also been identified as hotspots for various membrane receptors and signal transduction machineries (Pierce, 2002; Varshney et al., 2016).

Here, in order to capture the signaling events and immediate cellular responses triggered by BCR engagement, we took the approach to target APEX2 to the lipid raft domains of the plasma membrane by fusing a specific acylation sequence to the expression construct. As a result, we were able to track the changes occurring at the close proximity of the lipid raft domains, while the BCR rapidly gathered there upon activation. The high time-resolution of APEX2, 1 min, allowed us to dissect the dynamic changes in the lipid raft environment at the chosen time points of 5, 10 and 15 min of activation.

RESULTS

Generation of B cells with lipid raft domain targeted APEX2

In order to gain novel, spatiotemporal information about the various cellular responses to BCR activation, we aimed to target promiscuous APEX2 biotinylating enzyme to the close vicinity of BCR. Upon antigen binding, BCR is known to translocate from more fluid, detergent soluble plasma membrane domains to less fluid, detergent resistant membrane domains, also called lipid rafts (Sedwick & Altman, 2002; Varshney et al., 2016). We took advantage of this phenomenon and fused APEX2 with a specific lipidation tag to target the enzyme to the lipid raft domains in B cells and thereby report about the changes in the protein environment triggered by the BCR activation (Fig 1A). We fused a seven amino acid sequence (MGCVCSS) containing one myristoylation (Gly-2) and two S-acylation sites (Cys-3 and Cys-5) for palmitoylation, originally identified in the NH_2-terminus of Lck, to NH_2-terminus of APEX2. This myristoylation-palmitoylation-palmitoylation (MPP) sequence is responsible for the localization of Lck to the lipid rafts (Yasuda et al., 2000) and it has been shown to be able to target fusion proteins to the membrane, and to the immunological synapse of T cells (Bécart et al., 2008; Bi et al., 2001). In addition, we equipped our APEX2 construct with an mCherry fluorescent

protein (mCh) to facilitate the detection of APEX2 expression to generate the final construct MPP-mCh-APEX2 (Fig. 1B).

We transfected MPP-mCh-APEX2 into cultured A20 B cells, that already stably expressed transgenic hen egg lysozyme (HEL) -specific D1.3 IgM BCR (A20 D1.3) (Aluvihare et al., 1997), and generated a stable A20 D1.3 MPP-mCh-APEX2 cell line (Supplementary Fig. 1A). The flow cytometry analysis confirmed that mCherry$^+$ / IgM$^+$ cells composed >99% of the resulting cell line (data not shown).

To confirm that MPP-mCh-APEX2 indeed localizes to the plasma membrane, we first investigated its cellular localization using 3D AiryScan confocal microscopy (Huff, 2015) to gain sufficient resolution to unambiguously detect signals deriving from the B cell plasma membrane. The cells were settled on fibronectin-coated glass cover slips, fixed, and stained with wheat germ agglutinin (WGA) as a plasma membrane marker, and DAPI to mark the nuclei. MPP-mCh-APEX2 clearly colocalized with WGA demonstrating strong enrichment at the cell membrane (Fig. 1C). The lipid raft domains are typically very small in resting cells (Gupta & DeFranco, 2003) and transient in nature, making a microscopic detection of them highly challenging. However, upon activation, BCR translocates to the lipid rafts but concomitantly also forms clusters at the cell membrane. It is likely that, at the same time, these clusters represent larger, microscopically detectable, detergent resistant membrane domains (Gupta & DeFranco, 2003). Thus, we next activated the BCR and followed its colocalization with MPP-mCh-APEX2. We detected enrichment of both proteins together in the clusters at the cell membrane, indicating that upon BCR activation, the receptors are indeed enriched together with MPP-mCh-APEX2 (Fig. 1D).

To better investigate the membrane domain localization of MPP-mCh-APEX2, a flow cytometry-based assay was adopted (Gombos et al., 2004). We expressed MPP-mCh-APEX2 in A20 D1.3 cells together with model proteins resident either at lipid raft or detergent soluble membrane domains. The model protein for lipid rafts was glycosyl phosphatidylinositol (GPI) -anchored decay-accelerating factor fused to GFP (GPI-DAF-GFP) (Legler et al., 2005) and the model protein for detergent soluble membranes was a transmembrane domain from influenza virus hemagglutinin fused to GFP (TDM-GFP) (J et al., 2010). In this assay, the cells expressing MPP-mCh-APEX2 together with either raft or non-raft model proteins, were treated with 0.1 % Triton X-100 to release the detergent soluble proteins from the plasma membrane and the fluorescence was detected by flow cytometry. The fluorescence of MPP-mCh-APEX2 and the model proteins were compared before and after Triton X-100 treatment and the Detergent Resistance Index was calculated. The analysis showed that a considerable fraction of MPP-mCh-APEX2 resisted the detergent treatment although slightly less so than the GPI anchored model protein (Supplementary Fig 2A-B). The detergent soluble model protein,

on the other hand, was almost completely removed from the plasma membrane by the detergent. In the same experiment, we also stained the cells with non-stimulatory Fab fragments of anti-IgM antibodies to stain the BCR which were then activated using the model antigen HEL. Consistent with previous studies (Gupta & DeFranco, 2003), we saw that IgM substantially shifted towards detergent resistant membrane domains upon cell activation. This analysis provided important support to our approach to use lipid raft-preferring MPP-mCh-APEX2 as a proxy to label proteins enriching at the vicinity of signaling BCRs.

Prior to committing to the mass spectrometry assays we went on to exclude possible negative effects of the expression of Myr-mCh-APEX2 in B cells. We verified normal expression levels of IgM BCR in our A20 D1.3 MPP-mCh-APEX2 cells (data not shown). BCR was also internalized at normal kinetics upon receptor stimulation (data not shown). Also, the cells showed indistinguishable activation of the BCR-induced phosphorylation, detected by anti-phospho-Tyr antibodies, as compared to the parental cell line (Fig1E and Supplementary Fig. 1C).

Triggering of the biotinylation activity of APEX2 requires activation of the biotinylation reaction by addition of 1 mM H_2O_2 for 1 min. As it has been shown that H_2O_2 can inhibit protein phosphatases and thereby practically trigger receptor downstream signaling (Reth, 2002; Wienands et al., 1996), we examined the possible effects of H_2O_2 treatment in our experimental setup. We detected no increase in general protein phosphorylation upon incubation of cells with 1 mM H_2O_2 for 1 min, the conditions used to trigger biotinylation by APEX2, while ten times higher concentration of H_2O_2 induced profound signaling, consistent with previous reports (Reth, 2002) (Fig 1 F). This data suggests that there is no significant phosphorylation occurring in B cells during the 1min treatment with 1mM H_2O_2 despite of the potential of the treatment to generally inhibit protein phosphatases. We, thus, considered it unlikely that the H_2O_2 treatment would cause significant changes in the protein repertoire localizing at the lipid raft proximity, the target of our APEX2-mediated biotinylation approach.

Identification of B cell membrane-proximal proteome

To identify the proteins driving the immediate cellular responses to BCR activation, we devised an experimental setup to compare the proteomes at the vicinity of the plasma membrane in non-activated B cells and cells activated via their BCRs. As shown above, we targeted the biotinylating enzyme APEX2 to the plasma membrane, where it prefers detergent resistant membrane domains. These domains grow in size and enrich with BCRs upon receptor activation, allowing comparisons of the resting plasma membrane proximal proteome and the proteome enrich at the sites of activated

BCRs (Fig 1A). The cells, supplemented with biotin-phenol, were activated or not with potent surrogate antigen, $F(ab')_2$ fragments of anti-IgM antibodies for 5, 10 or 15 min. The biotinylation was triggered for the last minute of the assay by addition of 1mM H_2O_2 (Fig. 2A). The efficiency of biotinylation was verified in each set of samples by flow cytometric analysis, which typically showed biotinylation in ≈70% of cells. Lysed cells were subjected for streptavidin affinity purification to pull down the biotinylated proteins for mass spectrometry (MS) analysis (Fig 2A-B). To control the possible baseline activity of the APEX2 and the levels of endogenous biotinylation, samples without H_2O_2, or no biotin-phenol, were used, respectively. All samples were performed in triplicates (Hung et al., 2016). Trypsin-digested samples were analyzed by LC-ESI-MS/MS using nanoflow HPLC system (Easy-nLC1200, Thermo Fisher Scientific) coupled to the Orbitrap Fusion Lumos mass spectrometer and peptide/protein calling was done with MaxQuant software (Cox & Mann, 2008). Differential analysis was done using NormalyzerDE (Willforss et al., 2019). After filtration of known contaminants and background, we found 1677 proteins with 2 or more unique peptides identified (Supplementary file 1A).

The list of 1677 proteins contained high confidence hits from all experimental conditions together (Supplementary file 1B). As expected, we detected, with very high intensity values, several proteins reported to associate with lipid rafts (Fig 3A). However, the large number of total identified proteins illustrates the high efficacy of APEX2-mediated protein biotinylation in the vicinity of the enzyme, which allowed detection of also the cytosolic proteins as well as proteins resident at other membrane domains. In resting cells, detergent resistant membrane domains are very small and dynamic (Gupta & DeFranco, 2003) making it likely that also the proteins at the neighboring areas get efficiently labelled. Furthermore, the plasma membrane is probably not sharply divided in detergent resistant and soluble domains, but is expected to also contain also various areas with intermediate properties. Together with the 20nm radius of biotinylation, particularly in the resting conditions where the different membrane domains remain small and dynamic, MPP-mCh-APEX2 was expected to trigger vast labelling of the proteins close to the plasma membrane. Indeed, the proteome detected in non-activated B cells consisted of 1637 proteins (Fig. 3C, Supplementary file 1C 3), out of which 48 proteins were specific for resting cells (Fig. 3C, Supplementary file 1D). 40 additional proteins were specifically detected upon BCR activation (Fig. 3C and Supplementary file 1E).

We used GO cellular components analysis (Ashburner et al., 2000) and KEGG pathway assignment (Kanehisa et al., 2016) to gain information about the proteins identified in the full dataset. We identified highest protein counts in various cytoskeletal and membrane structures (Fig 3B), linked to fundamental functional pathways such as regulation of the actin cytoskeleton and endocytosis (Fig

3B). Importantly, from the more specific terms we found proteins significantly enriched to membrane rafts, immunological synapse and BCR signaling, providing confidence to our approach to detect changes in the protein environment linked to BCR signaling. The Supplementary file 1A lists all the identified proteins according to their intensity values to facilitate estimation of the protein abundance. The dataset is likely to cover a major fraction of the proteins resident at, and close to, the B cell plasma membrane and thereby provide highly useful large-scale information to promote future research.

Unexpectedly, we also identified a significant fraction of proteins linked to cellular events, such as regulation of transcription, translation and RNA transport, that are generally not associated to the vicinity of the plasma membrane. The presence of proteins linked to ribosomes function could relate to the potential activity of APEX2 right after protein synthesis but, interestingly, it has also been reported that various ribosomal proteins are palmitoylated and targeted to lipid rafts (Yang et al, 2010). This localization could to allow a new level of regulation of the protein synthesis activity. Ribosomal localization at the membrane could also explain the high significance of proteins linked to endoplasmic reticulum, RNA transport and ribonuclear protein granules (Fig. 3A). We also detected a substantial number of proteins linked to nuclear functions. Many of these proteins, like importin and exportin molecules, are shuffling between the cytoplasm and nucleus but some also are considered as nuclear resident proteins, such as nucleolin and histones. Notably, also nucleolin has been reported in an earlier MS study to be localized to the lipid rafts (Foster et al., 2003).

Lipid raft associated proteome

By analyzing the protein intensities between the samples and controls, similarly to Paek et al.(Paek et al., 2017), we first shortlisted proteins that are likely to be resident at the same membrane compartments with MPP-mCh-APEX2, i.e. to prefer detergent resistant membrane domains. We selected proteins that were at least log2 fold change >= 1.5 enriched in biotinylated samples of resting cells as compared to the control sample without triggering of biotinylation by H_2O_2. Additionally, we filtered out proteins that were enriched in samples from BCR-stimulated cells as compared to resting cells to only select protein that were constantly at the highest vicinity with MPP-mCh-APEX2. We identified 346 such proteins that we considered raft resident proteins (Fig. 3B, supplementary file 3A). The list contained both previously known and unknown lipid raft localized proteins. Surprisingly again, several proteins associated with ribosome, proteosome and nucleus, were included in the list. However, Martin et al. 2009 and Yang et al. 2010 had made similar discoveries. In their independent studies they discovered that some ribosomal and nuclear proteins undergo S-acylation modification that target them to the lipid raft domain in T cell hybridoma and DU145 cells respectively (Martin & Cravatt, 2009; Yang et al., 2010).

Proteins dynamics induced by BCR activation

In order to dissect the nature of changes occurring at the B cell plasma membrane upon BCR activation, we examined the differences in the biotinylated proteins at the vicinity of lipid rafts in different experimental conditions. Out of total of 1677 proteins identified, 1143 were common to all conditions. As a verification of our approach, we first looked into the components of the IgM BCR. Ighm, and IgK-V, the components of the transgenic IgM BCR activated in our setup, had greatly increased intensity, as quantified by MaxQuant, in activated samples (Supplementary file 2A Fig 4A and 4C). This provided further evidence that IgM translocates to the lipid raft domains, as expected, and supported the validity of our approach to capture changes in protein distribution upon BCR signaling. In contrast, Ighg, the heavy chain of IgG2a BCR, as well as Ig kappa chain C, which only binds IgG2a BCR in our cell line due to the chimeric nature of the transgenic IgM, remained unchanged upon receptor activation. Notably, however, IgG2a showed relatively high basal localization to lipid rafts. The lack of detectable dynamics in IgG2a localization would imply against any significant by-stander effects, at least in inter-isotype manner, that would change the behavior of also the un-ligated BCRs. Interestingly, despite of substantial enrichment of IgM heavy chain and kappa light chain to the lipid rafts upon activation, we saw decrease in the abundance of Igα and Igβ, proteins essential for the membrane stability of the BCR and its signal transmission. This important finding supports the model where the ratio of Igα/β and the BCR heavy chain is not fixed but can be tuned depending on the membrane location and/or the activation state. Our data suggests that upon cross-linking, perhaps facilitated by tighter molecular organization, IgM molecules could increasingly "share" their Igα/β sheath molecules decreasing the IgM:Igα/β ratio.

We then went on first to simply compare the proteins identified in different samples. Only 2 proteins, Kif20a/Mklp2 and Golga3, were found in all activation time points and not in any of the non-activated controls (Fig. 3C and table 1). The low number of these proteins probably reflects both the sensitivity of APEX2-mediated biotinylation, which leads to identification of also those proteins that are present at low levels, as well as the highly dynamic nature of the BCR activation in a manner where changes occurring at 5 minutes after activation can already be reset by 10 or 15 minutes. Indeed, we identified 9 proteins exclusively at 5 min, 4 proteins at 10 min, and 8 proteins at 15 min time points. 10 proteins were identified to be common for 5 and 10 min time points and 4 for 10 and 15 min time points (Fig. 3C).

On the other hand, we found 48 proteins to be exclusively present only in non-activated samples (Supplementary file 1D). This exclusion of quite a substantial set of proteins from the vicinity of lipid raft reflects the reorganization of the plasma membrane domains triggered upon BCR signaling. This is in agreement with the organization of signaling microclusters and coming together of smaller nanoclusters, lipid raft fusions etc (Gupta & DeFranco, 2003).

We then focused on the major part of our dataset, the proteins that were found present in all or most of the conditions. The protein abundance in each sample was obtained via intensity analysis using MaxQuant software. For statistical analysis of the changes in protein abundance at different conditions, we first applied criteria that the proteins need to be present in at least 12 out of total of 18 experimental samples, which restricted the analysis to 1258 proteins (Fig 2C, 4A-C and Supplementary file 2A). For the analysis, the missing values were then imputed using k-Neareast Neighbor (kNN) and quantitative differential analysis was done using NormalyzerDE (Willforss et al., 2019). The majority of the proteins did not undergo significant dynamics upon BCR activation but instead showed relatively stable abundance throughout different conditions. 213 proteins showed significant dynamicity with log2 fold change >= 1.5 enrichment upon cell activation (Fig. 4B Supplementary file 2B). Distinct sets of proteins were found to be enriched, or diminished, upon different time points. Only 7 proteins (Fig. 4A and B) were found significantly enriched in all time points of activation, while 75, 53, 55 proteins were significantly enriched at 5, 10 and 15 min time points, respectively (Fig 4B). This finding again underlines the fast kinetics of the cellular responses to BCR-signaling.

The dynamics of proteins linked to BCR signaling

We then focused on the cellular pathways with a previously reported, clear function in early B cell activation, BCR signaling and endocytosis, both of which were strongly represented in our data (Fig 3A). We inspected the dynamics within these groups as above. When analyzing the known components of the BCR signaling pathway, the results were somewhat unexpected. Various components of the signaling pathway did either not show significant dynamics, or they rather showed diminution while the IgM was translocating in.

Among the tyrosine kinases involved in BCR signaling that we identified were Lyn, Fyn, Blk and BTK. Lyn is often considered as one of the main kinases triggering BCR signaling, due to its early requirement to phosphorylate Igα/β ITAM motifs. Surprisingly, in this respect, we found Lyn diminished at the detergent resistant membrane domains upon BCR activation, although it has earlier

been reported to locate to the lipid rafts (Saeki et al., 2003; Sohn et al., 2008). However, the triggering of BCR signaling cascade is shared with Fyn, another Scr-family protein tyrosine kinase (Xu et al., Immunity 2005). In our data, Fyn shows higher abundance across the conditions and seems to be constantly located at the lipid-raft like regions. Notably, Lyn is also a critical negative regulator of BCR signaling, via its activatory function towards inhibitory phosphatases, SHP-1/2 and SHIP-1 (Xu et al., 2005). Our data supports the view that the main action of Lyn would be the regulatory function, which would occur mainly at the surroundings of the raft domains, where Lyn translocates upon BCR activation (Lamagna et al., 2014).

From the other components of the BCR signaling pathway, for example, activatory co-receptor CD19 did not show increased recruitment to the lipid rafts upon signal triggering (Figure 4C), but was constantly found in high abundance in all samples, suggesting localization in detergent resistant membrane domains. Another transmembrane protein closely linked to BCR activation but predominantly as a negative regulator, is a Siglec CD22. This sialic acid binding lectin was also found at the rafts in all conditions, yet, we noticed a peak in CD22 translocation to the lipid rafts at 5 min of activation followed by decline by 15min. This data would indicate that CD22 has a function at the close vicinity of the CR in the beginning of the signaling, although at later stages it gathers at more distant location. Our data augment previous study which shows that CD22 form a cap and translocate to the lipid raft domain following antigen stimulation (J. Yu et al., 2007). However, another study has shown that CD22 doesn't form cap nor translate to the lipid raft domain in primary B cells stimulated with hen egg lysozyme (HEL) (Pierce, 2002; Weintraub et al., 2000). Thus translocation of CD22 to the lipid raft seems to be dependent on how BCR is stimulated (J. Yu et al., 2007).

Also Btk, an important regulator of BCR downstream signaling showed increasing and strong negative fold-change upon activation, indicating exclusion from the forming BCR clusters in these settings. BTK is known to be recruited to the plasma membrane by PI(3,4,5)P_3 phosphoinositide, signaling lipid critical for B cell activation (Saito et al., 2001). Consistently, we detected a strong diminution of the regulatory subunit of PI3-kinase, Pik3r1, from the lipid rafts upon cell activation. This finding suggests early separation of the PI_3 -signaling from the actual location of BCR such that while the PI3-kinase is triggered fast after receptor engagement it might continue to function independently of physical vicinity of the BCR heavy and light chains. Also B cell linker (BLNK), a binding partner of BTK and various other BCR signaling proteins was downregulated at the rafts upon BCR signaling, although it showed substantial abundance throughout the samples. Phospholipase-γ2 (Plcγ2), that forms the other branch of lipid signaling downstream of BCR, was found constitutively strongly enriched at the lipid raft regions.

In summary, intriguingly, we found BCR signaling proteins mostly either non-dynamic raft-resident, or decreasing from the raft regions upon activation. IgM itself strongly translocated to the rafts, while the relative abundance of Igα/β decreased. Intriguingly, the data points towards early separation of signaling protein machineries from the BCR that is destined for endocytosis.

Proteins linked to endocytosis display dynamic behavior

Importantly, we found substantial dynamics of various proteins linked to BCR activation subsequent steps, such as cytoskeleton remodeling, endocytosis and membrane traffic, essential for internalization of BCR and further processing for antigen peptide presentation. Proteins linked to the remodeling of the actin cytoskeleton are a heterogenous group with multitude of functions. Similarly, we detected an array of various behaviors from recruitment to diminution from the lipid rafts upon activation (Fig. 4C). For example, an actin polymerization nucleator Wash1, linked to sorting of endosomal vesicles, was clearly enriched at 10 min after activation. A small GTPase Rap1 and adenylyl-cyclase associated protein 1 (Cap1), involved in positive regulation of actin polymerization, also showed enrichment at the same time point. On the other hand, coronin-1B, an organizer of cell leading edge actin polymerization was strongly diminished from the rafts at 15 minutes. An unconventional myosin Myo1g showed an interesting bipolar response, by getting first strongly enriched at 5 min time point, followed by a strong reduction at 15 min, while the non-muscle myosin-IIa, detected by myosin heavy chain-9 was enriched at 15 min.

Clathrin heavy chain 1 was highly abundant in all samples, while clathrin light chain A got increased at 5min after activation. Different clathrin adaptor proteins (AP) were detected in the dataset and showed differential abundance in the samples. Interestingly, AP2 subunits, primary family members linked to endocytosis, shower variable dynamics, such that AP2a1 was enriched at the early time points but diminished later, while AP2b1 got enriched at the later time points. This difference could reflect differential organization of the clathrin lattice or vesicle during the process. Interestingly, AP-1 complex subunit gamma-1, and AP-3 subunit beta-1, playing a role rather in intracellular vesicle sorting, both got increased upon activation, although with differential kinetics. An endocytosis regulator endophilin-B1 was excluded at 5 min but enriched at 15 min after activation.

Discussion

Signaling through the BCR is crucial for B cell's survival, proliferation and differentiation of B cells into plasma B cells (Liu et al., 2020). Despite extensive studies of BCR signaling using various techniques such as microscopy, proteomics, transcriptomic and molecular biology techniques, our understanding of the wealth of immediate and successive cellular changes occurring downstream of BCR activation is still poor. For such a complicated, multibranched response, large-scale approaches would be invaluable but are required to possess sufficient spatiotemporal resolution to account for the fast dynamics in the scale of minutes. Here, we employ proximity biotinylation proteomics based on lipid raft-targeted APEX2, to track at large scale the protein dynamics at the vicinity of the plasma membrane lipid raft regions, where BCR translocates upon activation. As APEX2 efficiently biotinylates its vicinity in the range of 20 nm in the time scale of 1 min, we believe it has significant power to report on signaling events at large scale in a highly time-resolved manner. By identifying over 1600 proteins, we draw a landscape of proteins at or close to the plasma membrane in B cells, and their dynamicity in respect to lipid rafts during BCR activation. In addition, we used this approach to propose proteins constitutively localized to the lipid raft domain of B cells.

The use of proximity labeling techniques provides an opportunity to elucidate the behaviors of various cellular machineries, in an unbiased manner, upon BCR activation. After facing challenges in fusing APEX2 to the Igα signaling subdomain of BCR, we decided to take advantage of the well-described translocation of the BCR to the lipid rafts upon activation and fused APEX2 with a lipidation sequence from Lck, that is known to target proteins to lipid rafts (Bécart et al., 2008; Bi et al., 2001). We postulate that this targeting implies low risk of amending the natural protein function, while still reporting about BCR vicinity in activating conditions with good accuracy. In non-activating conditions, the proteins locating at or close to lipid rafts in resting state get biotinylated. A vast majority of the proteins identified in the study were identified both in resting and activatory conditions. Among them was also the BCR. This can imply that the BCR is not present strictly in only either non-raft or raft domains domains, despite of differential enrichment. It is also important to note when interpreting the data in general that the rafts themselves are likely to be very small and dynamic in resting state and the division between the membrane subdomains is not clear-cut but there can be various "levels of raftness". Furthermore, BCR is expressed at very high levels on B cell surface and a substantial fraction of the receptors show significant mobility (Treanor et al., 2010). Considering this, it is not surprising to detect BCR also in the resting cells. Furthermore, only a very small fraction of the proteins that we detected were identified exclusively in one or some of the conditions. A few hundred of them showed condition-specific identification or enrichment profile. IgM BCR that was the most highly upregulated

protein upon cell activation that, at the same time, validated our approach to capture the BCR-proximal region upon cell activation. Notably, the majority of the proteins were identified at similar levels in all conditions indicating that their localization in respect to lipid rafts did not change.

Importantly, while the abundance of BCR (both Ighm and IgK-V) drastically increased at all-time points of BCR crosslinking, the known proteins involved in BCR signaling showed highly variable responses (Fig 4). We noticed reduction in abundance of, for instance LYN and BTK at the vicinity of lipid rafts upon BCR crosslinking. This would be consistent with LYN playing majorly negative regulatory role (Xu et al., 2005) after the BCR translocation to the rafts, while still perhaps initiating the signaling cascade before or at the time of translocation. On the other hand, we detected the family member FYN at all time points. FYN can carry out many of the functions of LYN (Xu et al., 2005), and perhaps is more dominant in the A20 B cell line we used. Intriguingly, we found overall slightly more proteins diminished upon signaling rather than enriched. We postulate that one of the underlying features affecting protein abundance in our system could be that in resting cells, due to the smaller size and probably more transient nature of lipid rafts, APEX2 biotinylation could be more likely to catch additional proteins in the surrounding non-raft regions. Upon BCR cross linking, rafts get bigger and more polarized, and the biotinylation might get more restricted to these specific domains. This feature could generate negative fold change for proteins locating to non-raft regions of the membrane or to the proteins without strong preference to the membrane domains.

We also utilized our setup to report on lipid raft resident proteins in B cells. For this, we used a similar strategy as Paek and colleagues (Paek et al., 2017), to filter out protein most likely constitutively very close to our APEX2 construct. One reason for identification of a protein, albeit with low intensity, in the control samples where biotinylation was not triggered with H_2O_2, could be a very close vicinity to the APEX2 that has a slight background activity. This reasoning is supported if the intensity then becomes drastically stronger when the H_2O_2 is applied and biotinylation triggered. We also further defined that the localization of the lipid raft resident proteins should not be significantly affected by BCR signaling. With these criteria, we identified 346 proteins to be raft resident. We then compared these proteins with proteins previously reported to be raft localized, and found 76 % of them in RAFTPROT database (Mohamed et al., 2019), providing good validation for the approach.

Somewhat unexpectedly, we also detected various nuclear proteins, ribosomal proteins and transcriptional proteins. Part of them could be explained by a possible residual fraction of MPP-mCh-APEX2 in the cytoplasm, on the way from the ribosomes to the plasma membrane, but some of them seemed specific to the lipid raft environment based on their high intensities or significant enrichment upon BCR cross-linking. Interestingly, the identification of many of these proteins could be explained

by direct targeting to the lipid raft membrane domains. Two independent studies, in T cell hybridoma and DU145 cells, suggested a set of ribosomal and nuclear proteins to undergo S-acylation and discovered their targeting to the lipid rafts of (Martin & Cravatt, 2009; Yang et al., 2010). In agreement with this, our list of lipid raft-resident proteins also contained many of these proteins. Moreover, increased tyrosine-phosphorylation of eIF3 complex proteins has been observed upon antigen stimulation of B cells (Matsumoto et al., 2009), suggesting that also some transcriptional proteins could be involved in BCR signaling. The possible unexpected relationships, suggested by our data, between the BCR signaling and proteins postulated to play a role in translational regulation, RNA transport and nuclear transport, are an interesting topic for future studies.

Our results provide an unbiased and comprehensive view, in a highly time-resolved manner, to the proteins and pathways that are triggered by BCR-stimulation. While many of the detected proteins are likely irrelevant for BCR signaling as the detection is simply based on spatial vicinity to MPP-mCh-APEX2, they draw a picture of the overall proteome at the B cell plasma membrane. The differential statistical analysis, with comparison of the proteomes of activated and resting B cells, reveals an interesting view with high temporal resolution and will be a valuable source of inspiration for future studies.

Materials and Methods

Design and cloning of Raft localized APEX2 constructs. pcDNA3-mito-APEX was a kind gift from Prof. Johanna Ivaska lab (University of Turku) and was used to create and PCR amplified APEX2 DNA. From here we created MPP-mCh-APEX2. Each MPP-mCh-APEX2 fusion protein has at the N-terminal seven amino acid sequence (MGCVCSS) that encodes the acylation sequence responsible for membrane localization of Lck, followed by mCherry sequence, V5 (GKPIPNPLLGLDST) epitope and then APEX2 sequence. MPP-mCh-APEX2 was then cloned into pcDNA™4/TO plasmid from Invitrogen (V1020-20).

Preparation of stable cell lines. pcDNA™4/Zeo/TO plasmid encoding MPP-mCh-APEX2 was transfected into A20 D1.3 cells line as previously described (Hernández-Pérez et al., 2019). In brief, 4 million cells were resuspended in 180 µl of 2S transfection buffer (5 mM KCl, 15 mM MgCl2, 15 mM HEPES, 50 mM Sodium Succinate, 180 mM Na2HPO4/ NaH2PO4 pH 7.2) containing 10 µg of plasmid and electroporated using AMAXA electroporation machine (program X-005, Biosystem) in 0.2 cm gap electroporation cuvettes. Cells were then transferred to 4ml of complete RPMI (cRPMI) containing extra 10 % FCS to recover overnight. Cells were then sorted single cell/well into 96 well flat bottom plates containing 100 µl of cRPMI supplemented with extra 10 % FCS using Sony SH800 Cell Sorter.

Cells were left to recover in cRPMI supplemented with extra 10 % FCS for 48 hrs before adding Zeocin (600 µg/ml final concentration). Clones expressing raft-mCherry-Apex2 were selected and expanded few weeks after sorting.

Proximity labeling Techniques. Frozen stable A20 D13 cells expressing MPP-mCh-APEX2 were recovered in a cRPMI without Zeocin for 48 hrs. After 48hrs, Zeocin was added and cells were allowed to multiply. Afterward cells were divided into the following conditions; activated: cells treated with 500uM biotin-phenol (BP) and activated with 10 µg of $F(ab')_2$ for 5, 10 or 15 min then 1 mM (final concentration) of H_2O_2 was added for 1 min; non-activated: cells treated with 500 µM BP for 45min, omitting $F(ab')_2$, and then adding 1 mM (final concentration) of H_2O_2 for 1 min; non-biotinylated control: cells treated with 500 µM BP , omitting $F(ab')_2$ and H_2O_2 and background control: cell treated only 1 mM H_2O_2 (final concentration) but omitting BP and $f(ab')_2$. After 1min H2O2 addition reaction were quenched with 2X quenching solution (20mM sodium ascorbate, 10 mM Trolox and 20 mM sodium azide solution in PBS). Cell were repeatedly washed 4 time with 1X quenching solution (10 mM sodium ascorbate, 5 mM Trolox and 10 mM sodium azide solution in PBS). To validate biotinylation we either used microscopy (Fig. 1D) and FACS (Supplementary Fid. 2A); where cells were fixed, permeabilized and stained with streptavidin 633 (Thermo Fischer Scientific) or western blot (Fig. 2B); where cells were lysed with modified RIPA buffer (50 mM Tris, 150 mM NaCl, 0.1% (wt/vol) SDS, 2 % OG, 0.5 % (wt/vol) sodium deoxycholate and 1 % (vol/vol) Triton X-100 in Millipore water, adjust the pH to 7.5 with HCl) and supplemented with 1× protease phosphatase inhibitor mini tablet from (Thermo Fisher Scientific, cat. no. A32961). After Lysis, lysate concentrations were measured using Pierce 660-nm protein assay reagent (Thermo Fisher Scientific, cat. no. 22660). Lysates were aliquot into 360ug of total protein, snap frozen and stored in -80°C.

Raft-Apex2 internalization Assay. Antigen internalization was done as previously described (Hernández-Pérez et al., 2019). Briefly, A20 D1.3 cells stably expressing MPP-mCh-APEX2 were stained on ice for 10 min with anti-IgM-biotin (Southern Biotech) and then washed with PBS. Afterward, Cells were incubated at 37°C and 5% CO_2 at different time points (0, 5, 15, 30, 45, 60 mins). For time 0min the cells were kept on ice throughout. After incubation, cells were kept on ice and stained with streptavidin-633 (LifeTechonologies #S-21375) for 20 min, washed and analyzed using BD LSR Fortessa.

Raft-Apex2 signaling Assay. A20 D1.3 cells expressing MPP-mCh-APEX2 were starved for 20 min (i. e resuspended in cRPMI without FCS). Cells were then incubated with either 10ug/ml of Fab2 or different concentration of H_2O_2 (0.1 mM, 1 mM, 10 mM and 100 mM) for 10 min. Afterward, cell were lysed with 2x SDS loading buffer. Lysed cells were sonicated and ran on SDS gel.

Detergent Resistance Membrane analysis by flow cytometry. A20D1.3 cells were transfected via electroporation with MPP-mCherry-APEX2 and GFP fused with GPI-anchored decay-accelerating factor (CD55) glycosyl phosphatidylinositol (DAF) (Legler et al., 2005) as a raft marker, or GFP fused to influenza virus hemagglutinin transmembrane domain (TDM) (J et al., 2010) as a non-raft marker. The assay was performed according to Gombos 2004. In short: 24 hours after transfection cells were incubated with Atto633-labeled Fab fragments of anti-mouse IgM on ice for 15 min, then the sample was split for activation with or wihtout 1ug/ml of HEL for 10 min at 37C, and precooled on ice for 5 min. Then the samples were divided for incubation in 0 or 0.1 % Triton-X100 in Imaging Buffer, 5 min on ice, to preserve or release the proteins bound to the lipid raft domains. Final concentration of 1 % of PFA was added and the cells were kept on ice until analyzed by flow cytometry. The parameter of detergent resistance was calculated:

$$\mathbf{DRI=(FL_{det}-FLBg_{det})/(FL_{max}-FLBg)}$$

where FL_{det} stands for fluorescence of the cells treated with detergent for 5 min, $FLBg_{det}$ for autofluorescence of the detergent-treated cells ,FL_{max} for fluorescence of labeled untreated cells (proportional to the protein expression level), FLBg for autofluorescence (background) of the unlabeled cells. The experiment was repeated at least 7 times for each marker in non-activated and 3times for activated version.

Microscopy. Glass bottom microscopy chambers (Mattek) were coated with 4ug/ml fibronectin in PBS for 1 h RT and washed with PBS. Cells were treated similarly to the mass spectrometry samples and, thus, incubated in 500 μM BiotinPhenol in complete medium at 37°C for 45 min. The cells were then let to settle on the microscopy chambers at 37°C for 15 min and incubated with 1 mM H_2O_2 together with 4% paraformaldehyde and 0.1 % glutaraldehyde to fix the sample, washed and continued to fix for further 10 min. Cells were washed, blocked in blocking buffer (BSA + goat serum) at RT for 1 h, labeled with Atto488-labelled WGA, washed, permeabilized with 0.1 % Triton X-100, at RT for 5 min, blocked again, and labeled with streptavidin-Atto/AF633 (1:2000) and DAPI at RT for 1 h. After washing, the samples were mounted in Vectashield. For visualization of MPP-mCherry-APEX2 upon BCR activation, after settling, 1 μg/ml of HEL antigen was added on ice, then incubated at 37°C for 5 min, and fixed for processing as above with exception of staining with aIgMFab2-Atto488 instead of WGA-Atto488. The AiryScan confocal microscopy was performed on Zeiss LSM880 microscope. *The profile intensity analysis was done in ZEN Blue software (version 3.1 Carl Zeiss Microscopy)*

Streptavidin pull-down of biotinylated proteins. 350 μg of whole lysate was incubated with 30μl of streptavidin magnetic beads (Pierce, cat. no. 88817) for 1hr at room temperature on a rotator.

Additional 500ul of RIPA buffer (50 mM Tris, 150 mM NaCl, 0.1 % (wt/vol) SDS, 0.5 % (wt/vol) sodium deoxycholate and 1 % (vol/vol) Triton X-100 in Millipore water. Adjust the pH to 7.5 with HCl) and supplemented with 1× protease phosphatase inhibitor mini tablet) were added to each sample to aid rotation. Beads were pelleted using magnetic rack and supernatant discarded. Beads were washed thrice with 1ml RIPA buffer for 5min each, twice with 1 ml 1 M KCl for 5 min each, twice with 1 ml 0.1 M Na2CO3 for 5min each, once with 1 ml 4 M urea in 10 mM Tris-HCl pH 8.0 for 5 min, once with 1 ml 4 M urea in 10 mM Tris-HCl pH 8.0 containing 50 µM biotin for 5min and thrice with 1 ml RIPA buffer for 5min each. All wash buffers were kept on ice at all time.

Biotinylated proteins were eluted with by boiling beads in 30 µl of 3× protein loading buffer supplemented with 2 mM biotin and 20 mM DTT for 10 min.

In-gel Digestion. Following elution, elutes were run on 10% SDS gel and gel stained with SimplyBlue SafeStain (ThermoFisher Scientific, cat. no. LC6065). Each gel lane was cut into 4 pieces and then digested as follow. Gel pieces were washed twice with 200 µl of 0.04 M NH_4HCO_3/ 50 % Acetonitrile (CAN). Then dehydrated with 200ul 100% ACN. Afterward, gels pieces were rehydrated in in 200 µl of 20 mM DTT and then dehydrated again as above. Gel pieces were again rehydrated with 100 µl 55 mM Iodoacetamide for 20 min in the dark RT, washed twice with 100ul 100mM NH_4HCO_3. Then dehydrated as above. 30 ‹l of 0.02 µg/ul of trypsin (Promega V5111) solution was added to gel pieces for 20 min followed by addition of 60µl solution containing 40 mM NH_4HCO_3/10 % ACN to completely cover the gel pieces and incubated at 37°C for 18 hrs. Peptides were then extracted using 90 µl of ACN followed by 150 µl of 50 % ACN / 5% HCOOH at 37°C for 15 min.

Mass spectrometry analysis. Mass spectrometry analysis was performed at the Turku Proteomics Facility, University of Turku and Åbo Akademi University. The facility is supported by Biocenter Finland. Data were collected by LC-ESI-MS/MS using a nanoflow HPLC system (Easy-nLC1200, ThermoFisher Scientific) coupled to the Orbitrap Fusion Lumos mass spectrometer (Thermo Fisher Scientific, Bremen, Germany) equipped with a nano-electrospray ionization source. Peptides were first loaded on a trapping column and subsequently separated inline on a 15 cm C18 column. A linear 20 min gradient from 8 to 39 % was used to elute peptides. MS data was acquired using Thermo Xcalibur 3.1 software (Thermo Fisher Scientific). A data dependent acquisition method that consist comprising an Orbitrap MS survey scan of mass range 300-2000 m/z followed by HCD fragmentation was used.

Protein Identification. The raw MS data were processed using MaxQuant software version 1.6.0.1 (Cox & Mann, 2008). MS/MS spectra were searched against mouse UniProt (reviewed (Swiss-Prot)) database **(**released September 2019) using Andromeda search engine (Cox et al., 2011). The following

configuration were used for MaxQuant search: Digestion set to trypsin, maximum number of missed cleavage allowed was set to 2, fixed modification set to Carbamidomethyl and variable modifications are N-terminal acetylation and methionine oxidation. Peptide and protein false discovery rate were set to 0.01. Match between runs was enabled. MaxLFQ that enables determination of relative intensity values of proteins and also normalize proteins intensity between samples was enabled but not used in downstream analysis (Cox et al., 2014). After MaxQuant run, 2526 proteins were identified. Afterward, contaminants and reverse hits were removed. For further analysis only proteins identified with at least 2 unique peptides (1677 proteins) were considered identified. The 1677 identified proteins were then classified using both KEGG pathway analysis (Fig. 3A) (Kanehisa et al., 2016) and gene ontology classification (Fig3B) (Ashburner et al., 2000) . Proteomic data set used in this paper will submitted to PRIDE (Vizcaíno et al., 2016).

Proteomics and differential enrichment analysis. Normalization and differential enrichment analysis were done using NormalyzerDE (Willforss et al., 2019) tools in Bioconductor. Quantile normalization was selected as the best normalization method following comparison of various normalization methods in NormalyzerDE. Prior to normalization and differential expression analysis, identified proteins with missing values in at least 7 conditions out of 18 conditions were filtered out. Afterward, missing value imputation was done using k-Neareast Neighbor (kNN) Imputation. Differential enrichment analysis was done using NormalyzerDE with statistical comparison method set to limma.

Following differential analysis we sought to identify proteins that are likely raft residence. Using similar strategy used by Paek et al., 2017, we first selected proteins with at least 1.5 log2 fold change in non-activated biotinylated sample compared to control samples (sample without H_2O_2 triggered biotinylation). Afterward we filter out proteins that are differentially enriched in $F(ab')_2$ stimulated biotinylated sample compared to non-activated biotinylated sample. It then remains 346 likely raft residence proteins.

Bioinformatics analysis. All downstream analysis were down with R. Enhancedvolcano was used to generate volcano plots (Blighe, K, S Rana, 2018). Enrichment analysis was done using R clusterProfiler package (G. Yu et al., 2012). UpSet plot was constructed to show intersect between conditions. A Venn diagram was constructed to depict intersect of proteins significantly enrich upon BCRs crosslink at different time point.

Acknowledgements

We thank Laura Grönfors and Citarra Burrows for technical help. Anne Rokka and staff at Turku Bioscience proteomic facility is acknowledged for their help in mass spectrometry analysis.

References

1. Aluvihare, V. R., Khamlichi, A. A., Williams, G. T., Adorini, L., & Neuberger, M. S. (1997). Acceleration of intracellular targeting of antigen by the B-cell antigen receptor: Importance depends on the nature of the antigen-antibody interaction. *EMBO Journal*, *16*(12), 3553–3562. https://doi.org/10.1093/emboj/16.12.3553
2. Ashburner, M., Ball, C. A., Blake, J. A., Botstein, D., Butler, H., Cherry, J. M., Davis, A. P., Dolinski, K., Dwight, S. S., Eppig, J. T., Harris, M. A., Hill, D. P., Issel-Tarver, L., Kasarskis, A., Lewis, S., Matese, J. C., Richardson, J. E., Ringwald, M., Rubin, G. M., & Sherlock, G. (2000). Gene ontology: Tool for the unification of biology. In *Nature Genetics* (Vol. 25, Issue 1, pp. 25–29). Nature Publishing Group. https://doi.org/10.1038/75556
3. Bécart, S., Canonigo Balancio, A. J., Charvet, C., Feau, S., Sedwick, C. E., & Altman, A. (2008). Tyrosine-Phosphorylation-Dependent Translocation of the SLAT Protein to the Immunological Synapse Is Required for NFAT Transcription Factor Activation. *Immunity*, *29*(5), 704–719. https://doi.org/10.1016/j.immuni.2008.08.015
4. Bi, K., Tanaka, Y., Coudronniere, N., Sugie, K., Hong, S., van Stipdonk, M. J., & Altman, A. (2001). Antigen-induced translocation of PKC-theta to membrane rafts is required for T cell activation. *Nature Immunology*, *2*(6), 556–563. https://doi.org/10.1038/88765
5. Blighe, K, S Rana, and M. L. (2018). *EnhancedVolcano: Publication-ready volcano plots with enhanced colouring and labeling.* https://github.com/kevinblighe/EnhancedVolcano
6. Cox, J., Hein, M. Y., Luber, C. A., Paron, I., Nagaraj, N., & Mann, M. (2014). Accurate proteome-wide label-free quantification by delayed normalization and maximal peptide ratio extraction, termed MaxLFQ. *Molecular & Cellular Proteomics: MCP*, *13*(9), 2513–2526. https://doi.org/10.1074/mcp.M113.031591
7. Cox, J., & Mann, M. (2008). MaxQuant enables high peptide identification rates, individualized p.p.b.-range mass accuracies and proteome-wide protein quantification. *Nature Biotechnology*, *26*(12), 1367–1372. https://doi.org/10.1038/nbt.1511
8. Cox, J., Neuhauser, N., Michalski, A., Scheltema, R. A., Olsen, J. V, & Mann, M. (2011). Andromeda: a peptide search engine integrated into the MaxQuant environment. *Journal of Proteome Research*, *10*(4), 1794–1805. https://doi.org/10.1021/pr101065j

9. Doerr, A. (2018). Proximity labeling with TurboID. *Nature Methods*, *15*(10), 764. https://doi.org/10.1038/s41592-018-0158-0
10. Foster, L. J., De Hoog, C. L., & Mann, M. (2003). Unbiased quantitative proteomics of lipid rafts reveals high specificity for signaling factors. *Proceedings of the National Academy of Sciences of the United States of America*, *100*(10), 5813–5818. https://doi.org/10.1073/pnas.0631608100
11. Gupta, N., & DeFranco, A. L. (2003). Visualizing Lipid Raft Dynamics and Early Signaling Events during Antigen Receptor-mediated B-Lymphocyte Activation. *Molecular Biology of the Cell*, *14*(2), 432–444. https://doi.org/10.1091/mbc.02-05-0078
12. Hernández-Pérez, S., Vainio, M., Kuokkanen, E., Šuštar, V., Petrov, P., Forstén, S., Paavola, V., Rajala, J., Awoniyi, L. O., Sarapulov, A. V, Vihinen, H., Jokitalo, E., Bruckbauer, A., & Mattila, P. K. (2019). B cells rapidly target antigen and surface-derived MHCII into peripheral degradative compartments. *Journal of Cell Science*, *133*(5). https://doi.org/10.1242/jcs.235192
13. Huff, J. (2015). The Airyscan detector from ZEISS: confocal imaging with improved signal-to-noise ratio and super-resolution. *Nature Methods*, *12*(12), i–ii. https://doi.org/10.1038/nmeth.f.388
14. Hung, V., Udeshi, N. D., Lam, S. S., Loh, K. H., Cox, K. J., Pedram, K., Carr, S. A., & Ting, A. Y. (2016). Spatially resolved proteomic mapping in living cells with the engineered peroxidase APEX2. *Nature Protocols*, *11*(3), 456–475. https://doi.org/10.1038/nprot.2016.018
15. Hung, V., Zou, P., Rhee, H.-W., Udeshi, N. D., Cracan, V., Svinkina, T., Carr, S. A., Mootha, V. K., & Ting, A. Y. (2014). Proteomic Mapping of the Human Mitochondrial Intermembrane Space in Live Cells via Ratiometric APEX Tagging. *Molecular Cell*, *55*(2), 332–341. https://doi.org/10.1016/j.molcel.2014.06.003
16. J, N., S, S., E, B., N, J., S, E., A, P. P., M, S., R, V., M, V., & A, H. (2010). Hemagglutinin of influenza virus partitions into the nonraft domain of model membranes. *Biophysical Journal*, *99*(2), 489–498. https://doi.org/10.1016/j.bpj.2010.04.027
17. Kaewsapsak, P., Shechner, D. M., Mallard, W., Rinn, J. L., & Ting, A. Y. (2017). Live-cell mapping of organelle-associated RNAs via proximity biotinylation combined with protein-RNA crosslinking. *ELife*, *6*, e29224. https://doi.org/10.7554/eLife.29224
18. Kanehisa, M., Sato, Y., Kawashima, M., Furumichi, M., & Tanabe, M. (2016). KEGG as a reference resource for gene and protein annotation. *Nucleic Acids Research*, *44*(D1), D457–D462. https://doi.org/10.1093/nar/gkv1070
19. Kuokkanen, E., Šuštar, V., & Mattila, P. K. (2015). Molecular control of B cell activation and immunological synapse formation. *Traffic (Copenhagen, Denmark)*, *16*(4), 311–326.

https://doi.org/10.1111/tra.12257

20. Kwak, K., Akkaya, M., & Pierce, S. K. (2019). B cell signaling in context. *Nature Immunology*, *20*(8), 963–969. https://doi.org/10.1038/s41590-019-0427-9
21. Lam, S. S., Martell, J. D., Kamer, K. J., Deerinck, T. J., Ellisman, M. H., Mootha, V. K., & Ting, A. Y. (2015). Directed evolution of APEX2 for electron microscopy and proximity labeling. *Nature Methods*, *12*(1), 51–54. https://doi.org/10.1038/nmeth.3179 [doi]
22. Lamagna, C., Hu, Y., DeFranco, A. L., & Lowell, C. A. (2014). B Cell–Specific Loss of Lyn Kinase Leads to Autoimmunity. *The Journal of Immunology*, *192*(3), 919–928. https://doi.org/10.4049/jimmunol.1301979
23. Legler, D. F., Doucey, M.-A., Schneider, P., Chapatte, L., Bender, F. C., & Bron, C. (2005). Differential insertion of GPI-anchored GFPs into lipid rafts of live cells. *The FASEB Journal*, *19*(1), 73–75. https://doi.org/10.1096/fj.03-1338fje
24. Liu, W., Tolar, P., Song, W., & Kim, T. J. (2020). Editorial: BCR Signaling and B Cell Activation. *Frontiers in Immunology*, *11*, 45. https://doi.org/10.3389/fimmu.2020.00045
25. Martin, B. R., & Cravatt, B. F. (2009). Large-scale profiling of protein palmitoylation in mammalian cells. *Nature Methods*, *6*(2), 135–138. https://doi.org/10.1038/nmeth.1293
26. Matsumoto, M., Oyamada, K., Takahashi, H., Sato, T., Hatakeyama, S., & Nakayama, K. I. (2009). Large-scale proteomic analysis of tyrosine-phosphorylation induced by T-cell receptor or B-cell receptor activation reveals new signaling pathways. *Proteomics*, *9*(13), 3549–3563. https://doi.org/10.1002/pmic.200900011
27. Mick, D. U., Rodrigues, R. B., Leib, R. D., Adams, C. M., Chien, A. S., Gygi, S. P., & Nachury, M. V. (2015). Proteomics of Primary Cilia by Proximity Labeling. *Developmental Cell*, *35*(4), 497–512. https://doi.org/10.1016/j.devcel.2015.10.015 [doi]
28. Mohamed, A., Shah, A. D., Chen, D., & Hill, M. M. (2019). RaftProt V2: understanding membrane microdomain function through lipid raft proteomes. *Nucleic Acids Research*, *47*(D1), D459–D463. https://doi.org/10.1093/nar/gky948
29. Paek, J., Kalocsay, M., Staus, D. P., Wingler, L., Pascolutti, R., Paulo, J. A., Gygi, S. P., & Kruse, A. C. (2017). Multidimensional Tracking of GPCR Signaling via Peroxidase-Catalyzed Proximity Labeling. *Cell*, *169*(2), 338-349.e11. https://doi.org/S0092-8674(17)30347-1 [pii]
30. Pierce, S. K. (2002). Lipid rafts and B-cell activation. *Nature Reviews Immunology*, *2*(2), 96–105. https://doi.org/10.1038/nri726
31. Reth, M. (2002). Hydrogen peroxide as second messenger in lymphocyte activation. *Nature Immunology*, *3*(12), 1129–1134. https://doi.org/10.1038/ni1202-1129
32. Rhee, H.-W., Zou, P., Udeshi, N. D., Martell, J. D., Mootha, V. K., Carr, S. A., & Ting, A. Y. (2013).

Proteomic mapping of mitochondria in living cells via spatially restricted enzymatic tagging. *Science (New York, N.Y.)*, *339*(6125), 1328–1331. https://doi.org/10.1126/science.1230593

33. Roux, K. J., Kim, D. I., Raida, M., & Burke, B. (2012). A promiscuous biotin ligase fusion protein identifies proximal and interacting proteins in mammalian cells. *The Journal of Cell Biology*, *196*(6), 801–810. https://doi.org/10.1083/jcb.201112098
34. Saeki, K., Miura, Y., Aki, D., Kurosaki, T., & Yoshimura, A. (2003). The B cell-specific major raft protein, Raftlin, is necessary for the integrity of lipid raft and BCR signal transduction. *The EMBO Journal*, *22*(12), 3015–3026. https://doi.org/10.1093/emboj/cdg293
35. Saito, K., Scharenberg, A. M., & Kinet, J. P. (2001). Interaction between the Btk PH domain and phosphatidylinositol-3,4,5-trisphosphate directly regulates Btk. *The Journal of Biological Chemistry*, *276*(19), 16201–16206. https://doi.org/10.1074/jbc.M100873200
36. Samavarchi-Tehrani, P., Samson, R., & Gingras, A. C. (2020). Proximity dependent biotinylation: Key enzymes and adaptation to proteomics approaches. In *Molecular and Cellular Proteomics* (Vol. 19, Issue 5, pp. 757–773). American Society for Biochemistry and Molecular Biology Inc. https://doi.org/10.1074/mcp.R120.001941
37. Sedwick, C. E., & Altman, A. (2002). Ordered Just So: Lipid Rafts and Lymphocyte Function. *Science Signaling*, *2002*(122), re2.
38. Sohn, H. W., Tolar, P., & Pierce, S. K. (2008). Membrane heterogeneities in the formation of B cell receptor–Lyn kinase microclusters and the immune synapse. *Journal of Cell Biology*, *182*(2), 367–379. https://doi.org/10.1083/jcb.200802007
39. Treanor, B., Depoil, D., Gonzalez-Granja, A., Barral, P., Weber, M., Dushek, O., Bruckbauer, A., & Batista, F. D. (2010). The Membrane Skeleton Controls Diffusion Dynamics and Signaling through the B Cell Receptor. *Immunity*, *32*(2), 187–199. https://doi.org/10.1016/j.immuni.2009.12.005
40. Varshney, P., Yadav, V., & Saini, N. (2016). Lipid rafts in immune signalling: current progress and future perspective. *Immunology*, *149*(1), 13–24. https://doi.org/10.1111/imm.12617
41. Vizcaíno, J. A., Csordas, A., del-Toro, N., Dianes, J. A., Griss, J., Lavidas, I., Mayer, G., Perez-Riverol, Y., Reisinger, F., Ternent, T., Xu, Q.-W., Wang, R., & Hermjakob, H. (2016). 2016 update of the PRIDE database and its related tools. *Nucleic Acids Research*, *44*(D1), 447. https://doi.org/10.1093/nar/gkv1145
42. Weintraub, B. C., Jun, J. E., Bishop, A. C., Shokat, K. M., Thomas, M. L., & Goodnow, C. C. (2000). Entry of B Cell Receptor into Signaling Domains Is Inhibited in Tolerant B Cells. *The Journal of Experimental Medicine*, *191*(8), 1443–1448. https://www.ncbi.nlm.nih.gov/pmc/articles/PMC2193133/

43. Wienands, J., Larbolette, O., & Reth, M. (1996). Evidence for a preformed transducer complex organized by the B cell antigen receptor. *Proceedings of the National Academy of Sciences of the United States of America*, *93*(15), 7865–7870. https://doi.org/10.1073/pnas.93.15.7865
44. Willforss, J., Chawade, A., & Levander, F. (2019). NormalyzerDE: Online Tool for Improved Normalization of Omics Expression Data and High-Sensitivity Differential Expression Analysis. *Journal of Proteome Research*, *18*(2), 732–740. https://doi.org/10.1021/acs.jproteome.8b00523
45. Xu, Y., Harder, K. W., Huntington, N. D., Hibbs, M. L., & Tarlinton, D. M. (2005). Lyn tyrosine kinase: Accentuating the positive and the negative. In *Immunity* (Vol. 22, Issue 1, pp. 9–18). Cell Press. https://doi.org/10.1016/j.immuni.2004.12.004
46. Yang, W., Di Vizio, D., Kirchner, M., Steen, H., & Freeman, M. R. (2010). Proteome scale characterization of human S-acylated proteins in lipid raft-enriched and non-raft membranes. *Molecular & Cellular Proteomics: MCP*, *9*(1), 54–70. https://doi.org/10.1074/mcp.M800448-MCP200
47. Yu, G., Wang, L.-G., Han, Y., & He, Q.-Y. (2012). clusterProfiler: an R package for comparing biological themes among gene clusters. *Omics: A Journal of Integrative Biology*, *16*(5), 284–287. https://doi.org/10.1089/omi.2011.0118
48. Yu, J., Sawada, T., Adachi, T., Gao, X., Takematsu, H., Kozutsumi, Y., Ishida, H., Kiso, M., & Tsubata, T. (2007). Synthetic glycan ligand excludes CD22 from antigen receptor-containing lipid rafts. *Biochemical and Biophysical Research Communications*, *360*(4), 759–764. https://doi.org/10.1016/j.bbrc.2007.06.110

Figure Legends

Figure 1. Lipid raft targeted MPP-mCh-APEX2 accumulates together with BCR upon receptor activation. A) A schematic view of the chosen experimental system. Lipid raft localized APEX2 is targetedshowing translocation of BCR to lipid raft upon activation. APEX2 is targeted to the lipid raft membrane domains, where also BCR translocates upon activation. APEX2 induces biotinylation of proteins in the <20 nm range. This construct allows identification and label-free quantification of proteins proximal to the lipid rafts at different time points of BCR activation. **B)** A schematic showing the design of MPP-mCh-APEX2. **C)** A20 D 1.3 B cells expressing MPP-mCh-APEX2 were settled on a fibronectin-coated glass cover slips for 1 hr prior to fixation. Cells were stained with wheat germ agglutinin (WGA) as a membrane marker and dapi for nucleus. Airyscan super-resolution confocal microscopy was used to image mCherry (magenta), WGA (cyan) and dapi (white). A clear colocalization

of MPP-mCh-APEX2 and WGA was detected at the plasma membrane. **D)** A20 D 1.3 B cells expressing MPP-mCh-APEX2 were settled on a fibronectin-coated glass cover slips for 1 hr, activated (right), or not (left), by addition of 1 µg of HEL for 5 min, and fixed. The samples were stained for IgM and dapi was used to report on nucleus. Airyscan super-resolution confocal microscopy was used to image mCherry (magenta), IgM (cyan) and dapi (white). Upon activation IgM was found more dotted and the IgM dots were also enriched with MPP-mCh-APEX2. **E)** MPP-mCh-APEX2 expressing A20 D1.3 B cells were treated with 0, 0.1, 1 and 10 mM H_2O_2 for 1 min. Cells were lysed and subjected for Western blotting. The membranes were probed with HRP-anti phospho-Tyrosine antibodies, and anti β-actin as a loading control. **F)** Wild-type and MPP-mCh-APEX2 expressing A20 D1.3 B cells were stimulated with or without 10 µg of anti-IgM $F(ab')_2$ and subjected for Western blotting as in E).

Figure 2. Experimental design and flow of the analysis. A) A schematic representation of the experimental samples and controls analyzed by quantitative label-free MS in this study. Three different biological replicates were prepared for all conditions. Sample were treated with 500 µM BP or not, 1 mM H_2O_2 or not and 10 µg of anti-IgM $F(ab')_2$ or not. Biotinylated proteins were then enriched using magnetic streptavidin-coated beads and analyzed by LC-ESI-MS/MS. **B) Left**: MPP-mCh-APEX2 expressing A20 D1.3 B cells were supplemented with biotin-phenol and the biotinylation was triggered or not by adding 1 mM H_2O_2 for 1 min. The samples eluted from the streptavidin-coated beads were analysed with a Silver stained SDS-PAGE (left) and a Western blot probed with streptavidin-HRP. **C)** Flow chart that shows the filtering steps used for the data analysis.

Figure 3. Pathway analysis of the 1677 identified proteins. A) A KEGG pathway enrichment analysis shows cellular pathways enriched among the identified proteins. To remove redundancy in the identified pathways terms, pathway terms that had ≥ 50% similarities were grouped and only the one with lowest Adj. P-value was used. **B)** Classification of the identified proteins based on cellular component GO terms. To remove redundancy in the GO terms, GO terms that had ≥ 50% similarities were grouped and only the one with lowest Adj. P-value was used. **C)** An upset plot showing intersections among identified proteins. **D)** A table showing proteins identified only upon activation in (5, 10 and 15) min, (5 and 10) min, (5 and 15) min, (10 and 15) min, 5 min, 10 min and 15 min.

Figure 4. Enrichment analysis. A) Volcano plots illustrate identified protein dynamics upon anti-BCR activation at 5, 10 and 15 min. The data is based on the differential enrichment analysis of 1258 identified proteins (as in Fig 2C). **Upper left**: Non-activated Vs activated cells at 5 min. **Upper right**: Non-activated Vs activated cells at 10 min. **Lower left**: Non-activated Vs activated cells at 15 min. **Lower right**: Table of proteins that were found to be enriched in the activated cells at all-time points

with a log2 fold change > 1.5 and Adj. P-value < 0.05. Red dots: significant (Adj. P-Value<0.05) with a log2 fold change > 1.5. Blue dots: significant (Adj. P-Value<0.05) with a log2 fold change < 1.5. Green dots: not significant (Adj. P-Value>0.05) with a log2 fold change > 1.5. Black dots: not significant (Adj. P-Value>0.05) with a log2 fold change < 1.5. **B)** A venn diagram showing the numbers of significantly enriched proteins with log2 fold change >= 1.5 at different time points and their intersections. In total, 213 proteins. **C)** Heatmap of the enrichment of proteins classified to KEGG pathway of B cell activation.

Figure 5. Proposed raft resident proteins. A) Table of top 10 proteins with highest intensity among proposed raft resident proteins.

SUPPLEMENTARY FIGURES

Supplementary Figure 1. A) A schematic representation of flowcytometry assay to detect raft association of membrane proteins. Cells were treated with TritonX-100 detergent. Raft domain which is more detergent resistant is retains with its associated membrane proteins whereas non-raft domain is dissolved with detergent. **B)** Bar chart compares detergent resistance of MPP-mCh-APEX2 and IgM BCRs expressed in A20 D 1.3 cells upon activation with HEL or not with lipid raft markers (DAT-GPI) and non-raft marker (TMD-GFP). **C)** MPP-mCh-APEX2 expressing A20 D1.3 B cells and WT cells were treated with 0, 0.1, 1 and 10 mM H_2O_2, or 10ug anti-BCR. Cells were lysed and subjected for Western blotting. The membranes were probed with HRP-anti phospho-Tyrosine antibodies, and anti β-actin as a loading control.

Supplementary Figure 2: A) MPP-mCh-APEX2 expressing A20 D1.3 B cells were supplemented with biotin-phenol, activated or not with anti-BCR for 5min and the biotinylation was triggered or not by adding 1 mM H_2O_2 for 1 min. Cells were fixed with 4% PFA, permeabilzed and stained with streptavidin-633.

SUPPLEMENTARY FILES

Supplementary file 1. B cells lipid raft proteomic data. A) List of identified proteins after filtering out proteins with less than 2 unique peptides. **B)** List of proteins identified in resting MPP-mch-APEX2 expressing B cells. **C)** List of proteins identified exclusively in resting MPP-mch-APEX2 B cells. **D)** Proteins identified exclusively in activated samples.

Supplementary file 2. A) List of proteins quantified from different time point of activation of MPP-mch-APEX2 expressing A20 D 1.3 B cells with $F(ab')_2$. **B)** List of proteins that show significant enrichment at different time points and have2log2 fold change >=1.5

Supplementary file 3. A) List of proteins proposed to be likely lipid raft resident **B)** List of proteins common to our proposed raft resident proteins and RaftProt database (Mohamed et al., 2019).

Figure 1

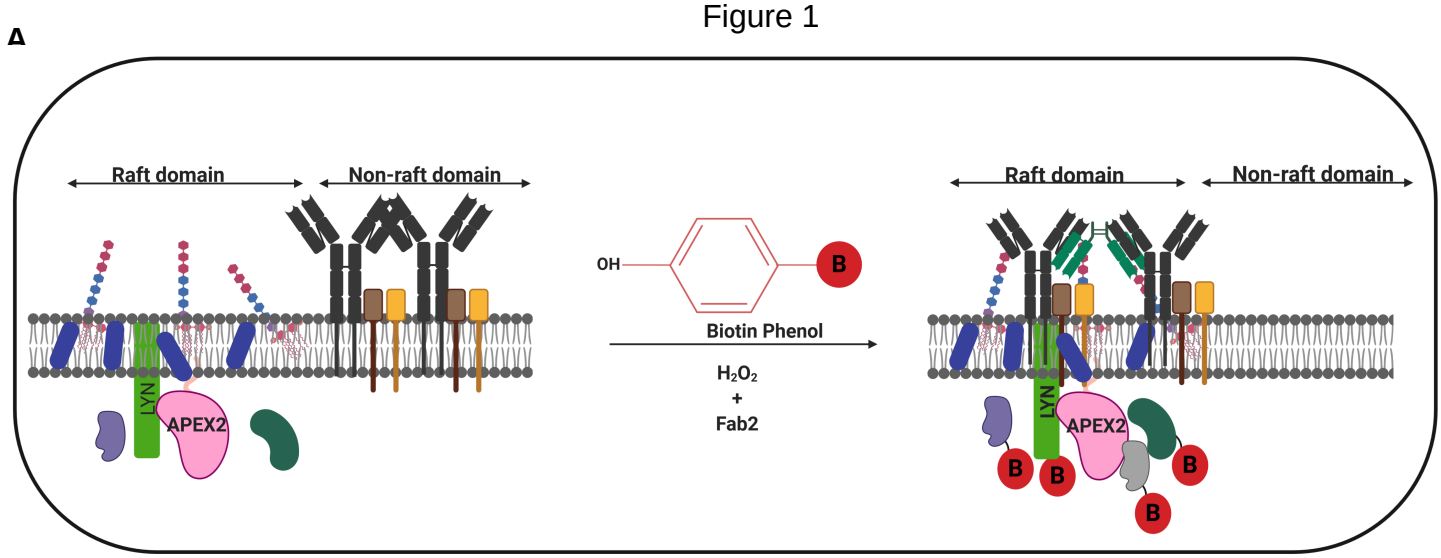
A
Raft domain
Non-raft domain
LYN
APEX2
OH
B
Biotin Phenol
H_2O_2
+
Fab2
Raft domain
Non-raft domain
LYN
APEX2
B
B
B
B

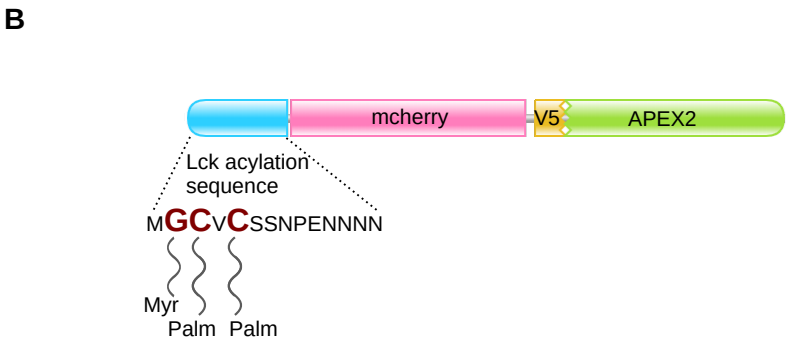
B
mcherry
V5
APEX2
Lck acylation sequence
MGCVCSSNPENNNN
Myr
Palm
Palm

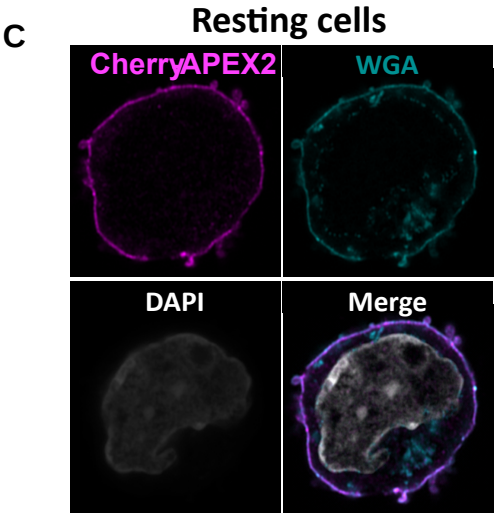
C
Resting cells
CherryAPEX2
WGA
DAPI
Merge

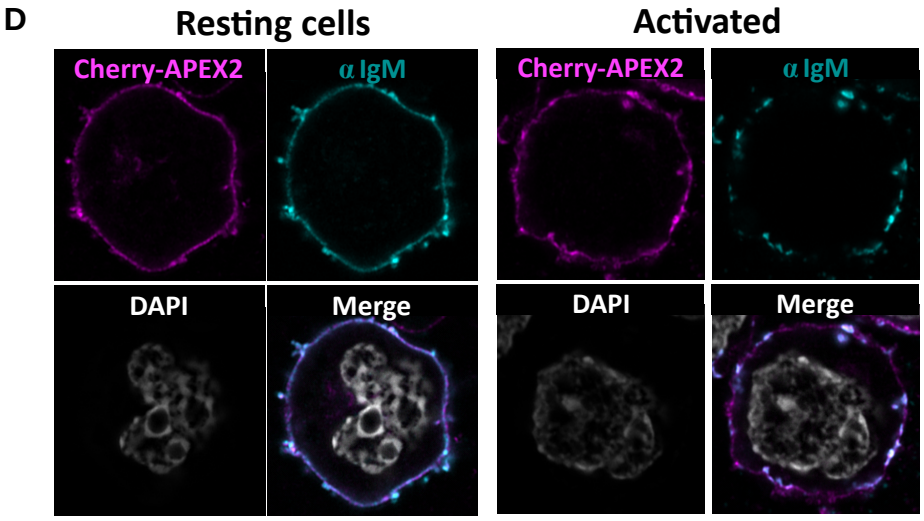
D
Resting cells
Activated
Cherry-APEX2
α IgM
Cherry-APEX2
α IgM
DAPI
Merge
DAPI
Merge

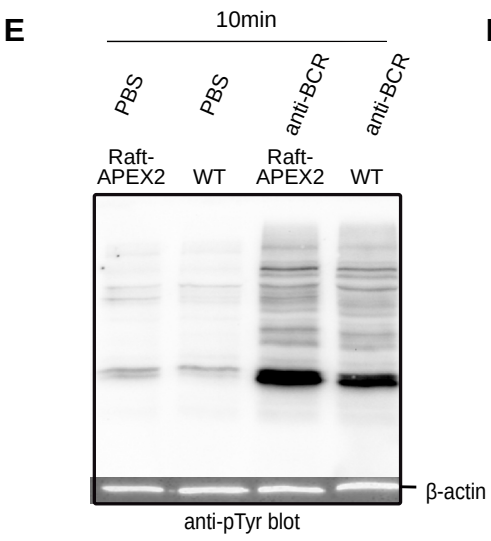
E
10min
PBS
PBS
anti-BCR
anti-BCR
Raft-APEX2
WT
Raft-APEX2
WT
β-actin
anti-pTyr blot

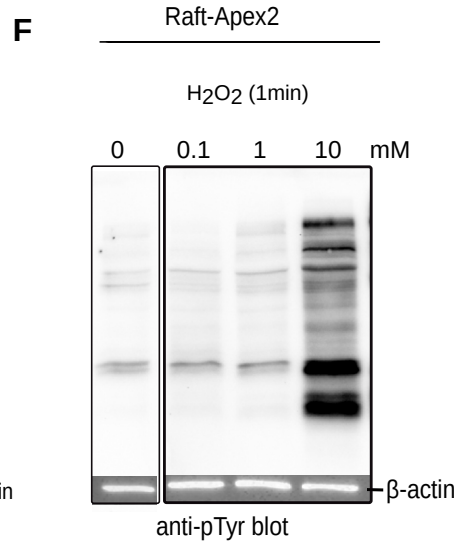
F
Raft-Apex2
H_2O_2 (1min)
0
0.1
1
10
mM
β-actin
anti-pTyr blot

Figure 2

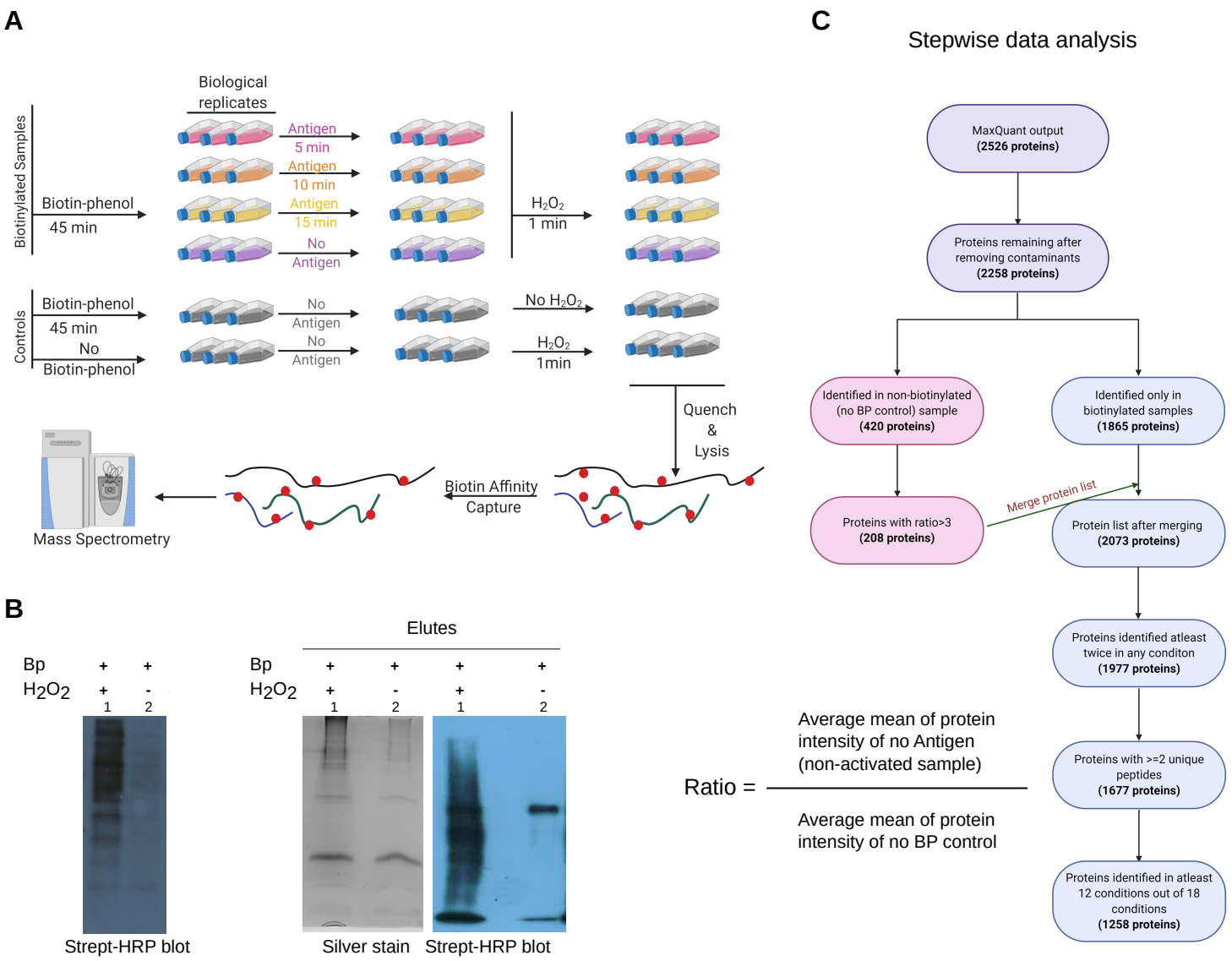
A
Biological replicates
Biotinylated Samples
Biotin-phenol
45 min
Antigen
5 min
Antigen
10 min
Antigen
15 min
No
Antigen
H_2O_2
1 min
Controls
Biotin-phenol
45 min
No
Biotin-phenol
No
Antigen
No
Antigen
No H_2O_2
H_2O_2
1min
Quench
&
Lysis
Biotin Affinity
Capture
Mass Spectrometry
B
Elutes
Bp + +
H_2O_2 + -
1 2
Bp + + + +
H_2O_2 + - + -
1 2 1 2
Strept-HRP blot
Silver stain
Strept-HRP blot
C
Stepwise data analysis
MaxQuant output
(2526 proteins)
Proteins remaining after removing contaminants
(2258 proteins)
Identified in non-biotinylated (no BP control) sample
(420 proteins)
Identified only in biotinylated samples
(1865 proteins)
Proteins with ratio>3
(208 proteins)
Merge protein list
Protein list after merging
(2073 proteins)
Proteins identified atleast twice in any conditon
(1977 proteins)
Proteins with >=2 unique peptides
(1677 proteins)
Proteins identified in atleast 12 conditions out of 18 conditions
(1258 proteins)
Ratio =
Average mean of protein intensity of no Antigen (non-activated sample)
Average mean of protein intensity of no BP control

Figure 3

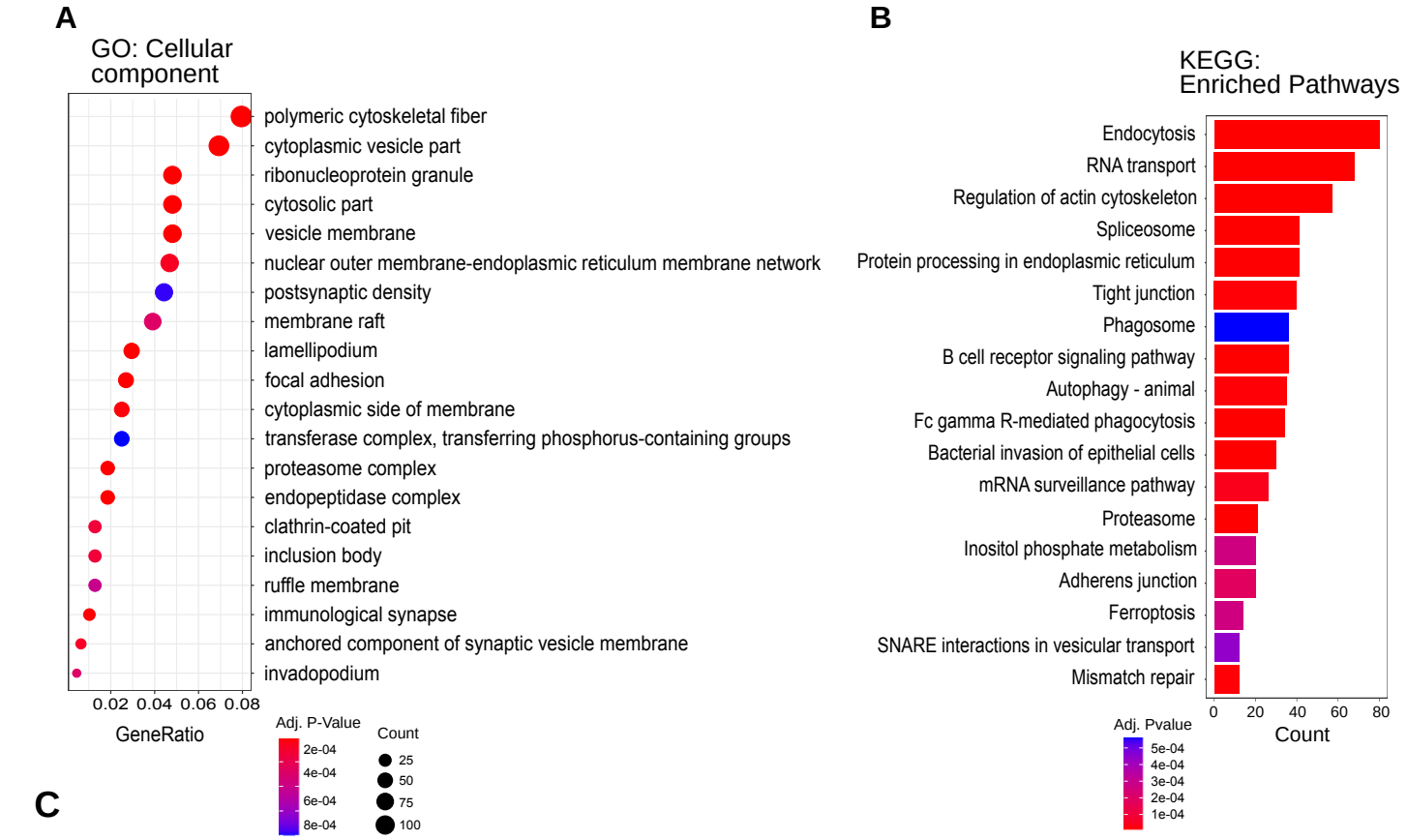

C

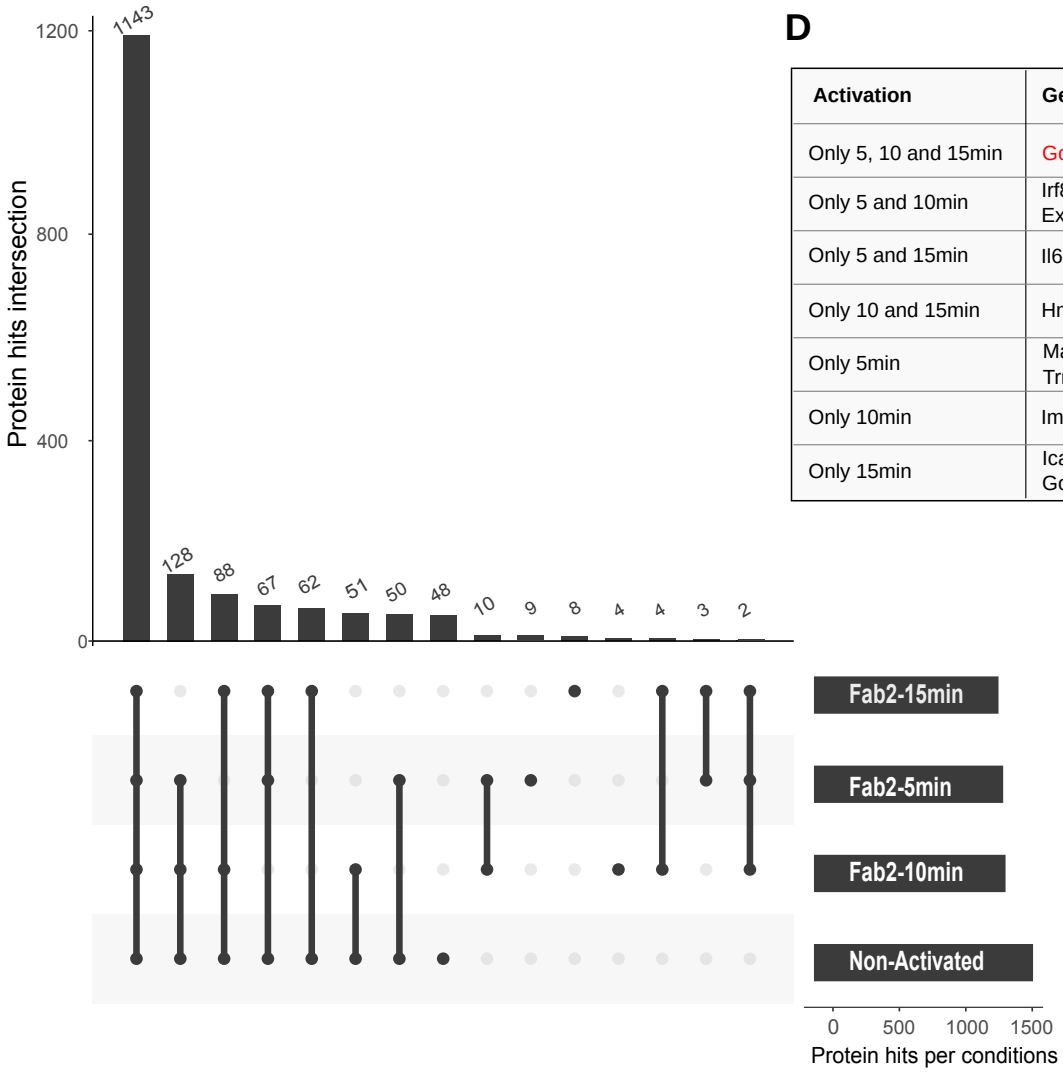

D

Activation	Gene names
Only 5, 10 and 15min	Golga3 and Kif20A
Only 5 and 10min	Irf8, Sec61a1, Csrp2, Xrn1, Cab39, Exosc3, Ttc27,Cdc34,Llph and Tollip
Only 5 and 15min	Il6st, Nt5dc1 and Riok2
Only 10 and 15min	Hmgb2, Ncor1, Ankib1 and Dcun1d5
Only 5min	Map3k15, Alad, Zzef1, Atg2b, Riox2, Trnt1, Rnf31, Emc3 and Dis3
Only 10min	Impdh1, Cep43, Ubxn7 and Tnfaip8
Only 15min	Icam1, Crnkl1, Cux1, C2cd2l, Septin11, Gorasp2, Ppid and Ak2

Figure 4

A

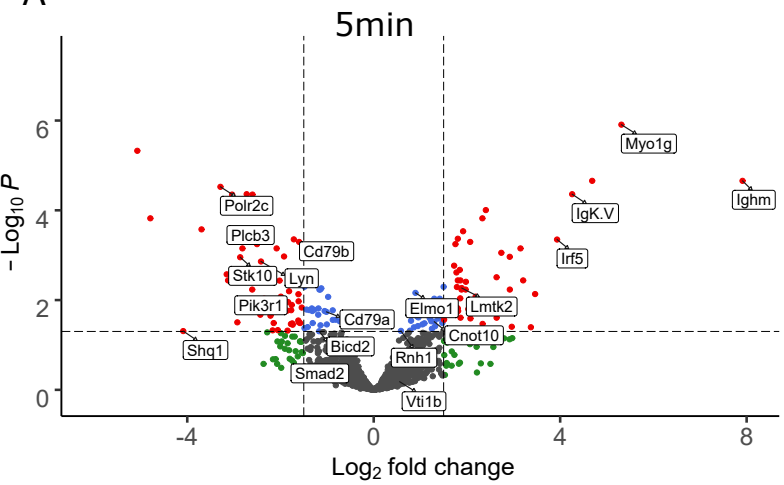

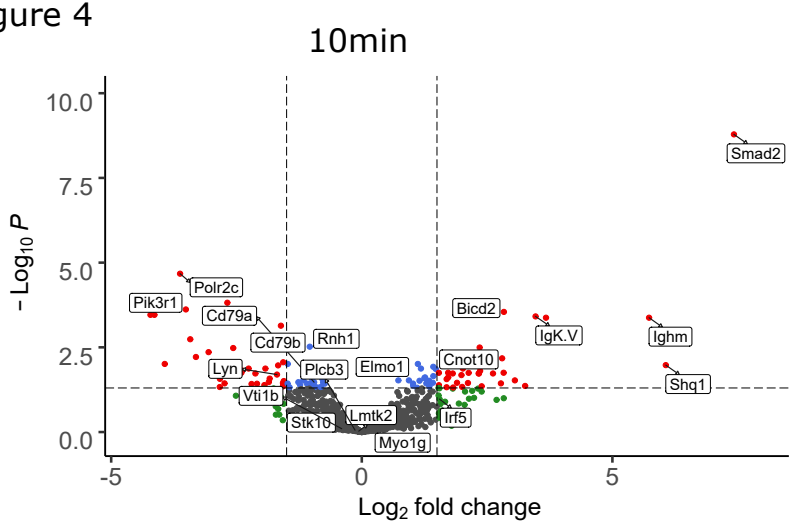

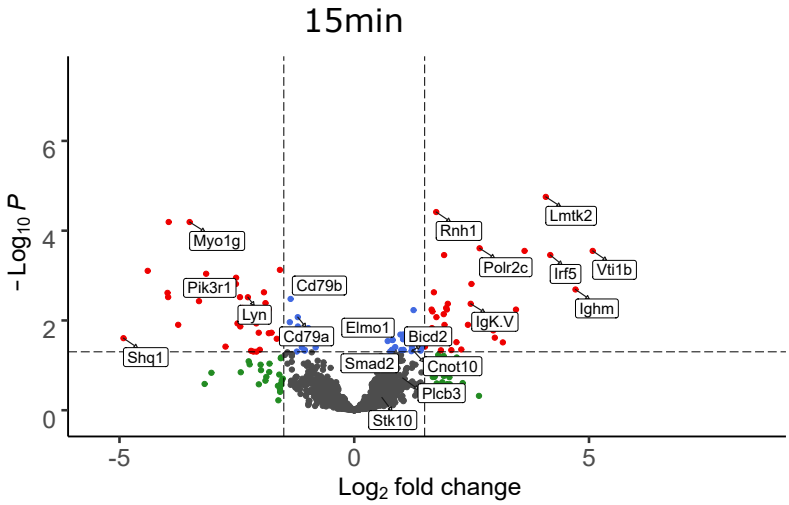

NS · Log_2 FC · p-value · p – value and $\log_2$ FC

List of protein enriched in all activated conditions

Gene names
IgK-V
Ighm
Lyn
Mark2
Pik3r1
Polr2c
Shq1

B

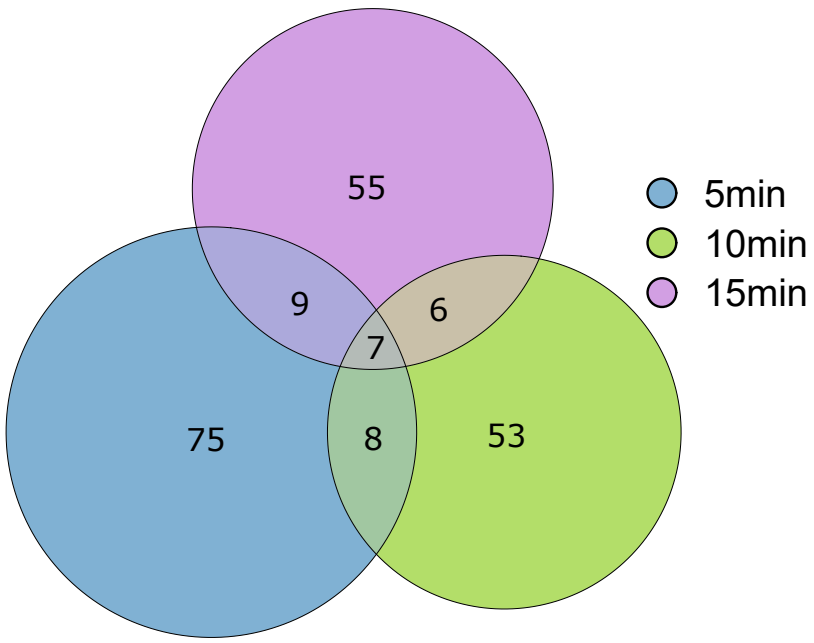

C

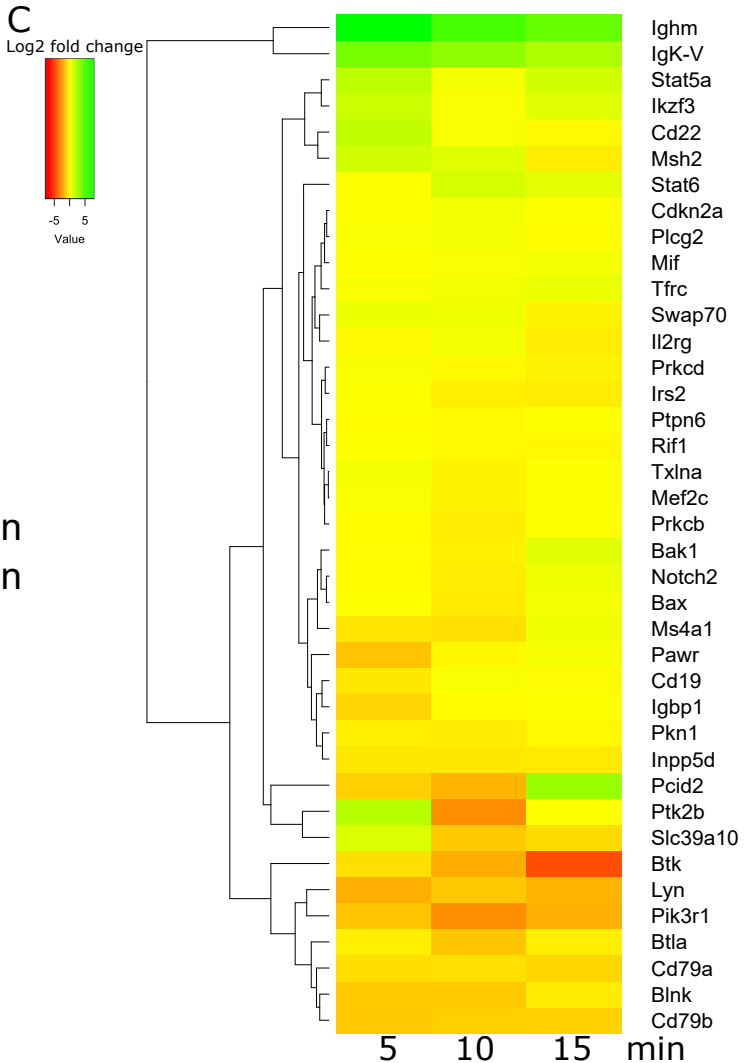

Figure 5

A

List of top proposed raft residence proteins

Gene names
Actb
Plekhn1
Tubb5
Hspa8
Prdx1
Ddx3x
Ezr
Rpl10
Iap
Eif4a1

Supplementary figure 1

A

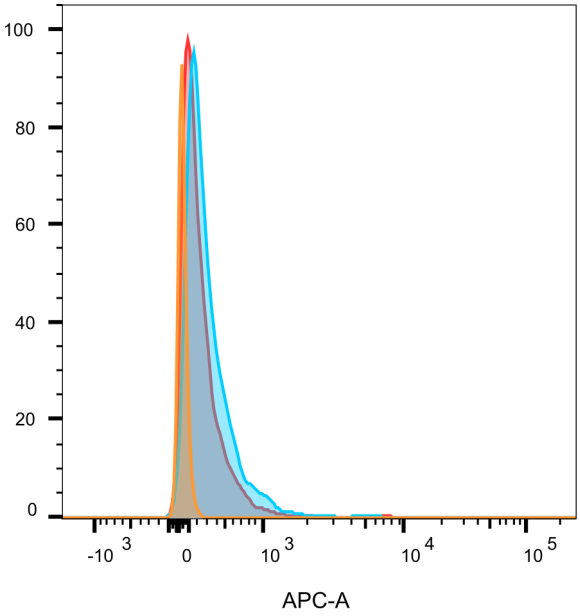

non-biotinylated control

non activated biotinylated sample

5min Fab2 activated biotinylated sample

Supplementary Figure 2

A

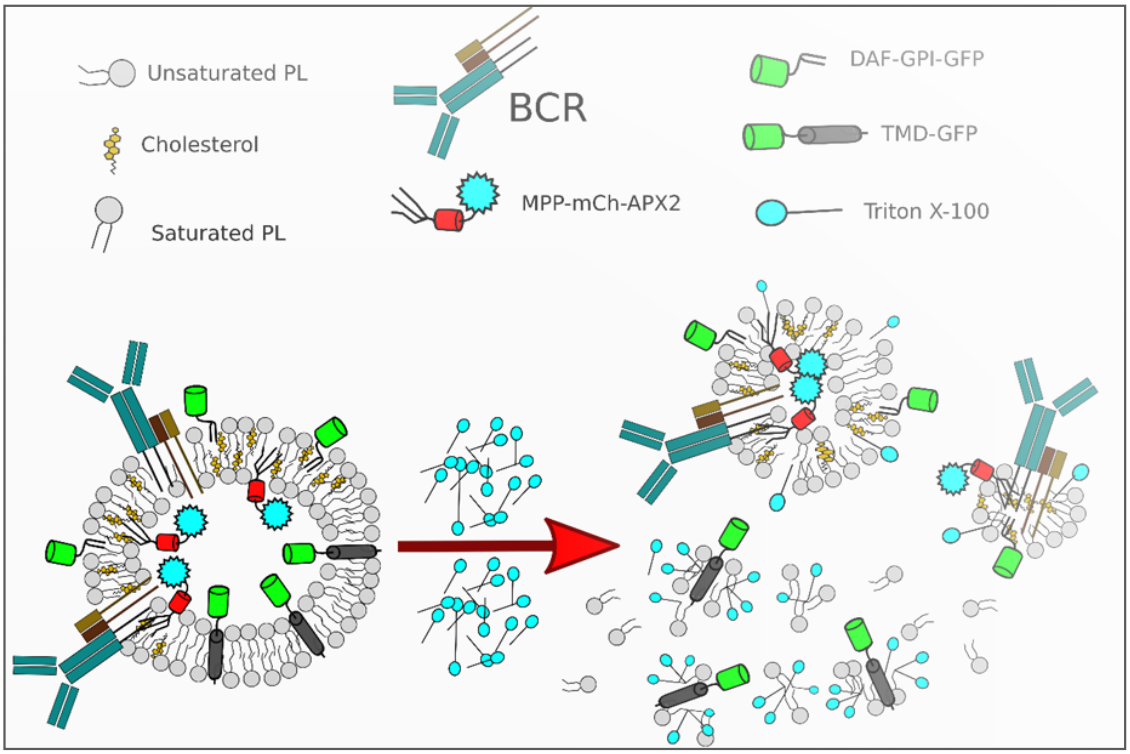

B

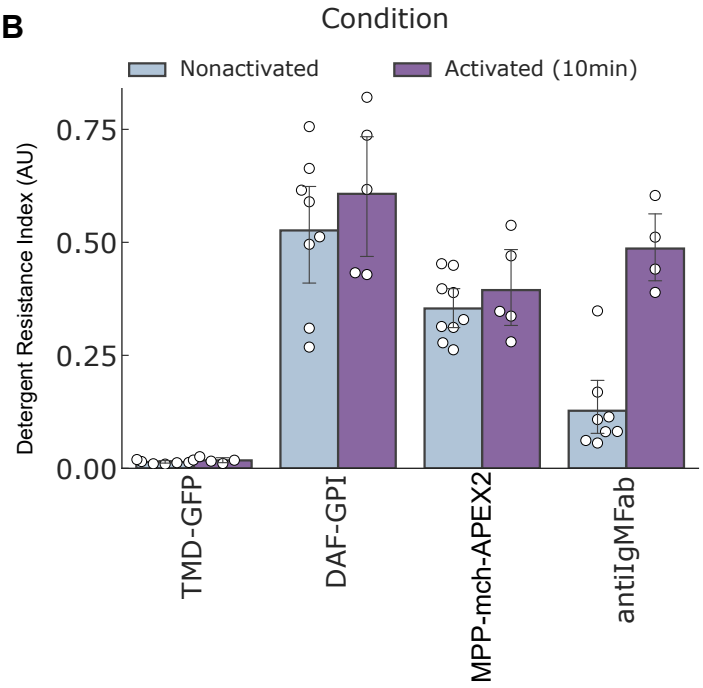
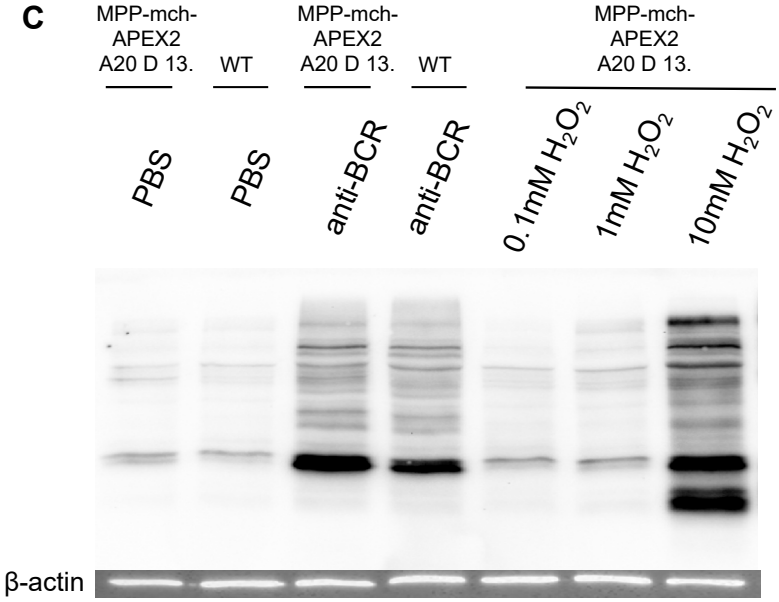
C